JOURNAL OF GEOPHYSICAL RESEARCH, VOL. 115, C00B17, doi:10.1029/2009JC005452, 2010

River Influences on Shelf Ecosystems: Introduction and synthesis

B. M. Hickey,[1] R. M. Kudela,[2] J. D. Nash,[3] K. W. Bruland,[2] W. T. Peterson,[4] P. MacCready,[1] E. J. Lessard,[1] D. A. Jay,[5] N. S. Banas,[6] A. M. Baptista,[7] E. P. Dever,[3] P. M. Kosro,[3] L. K. Kilcher,[3] A. R. Horner-Devine,[8] E. D. Zaron,[5] R. M. McCabe,[9] J. O. Peterson,[3] P. M. Orton,[10] J. Pan,[5] and M. C. Lohan[11]

Received 21 April 2009; revised 23 July 2009; accepted 26 August 2009; published 3 February 2010.

[1] River Influences on Shelf Ecosystems (RISE) is the first comprehensive interdisciplinary study of the rates and dynamics governing the mixing of river and coastal waters in an eastern boundary current system, as well as the effects of the resultant plume on phytoplankton standing stocks, growth and grazing rates, and community structure. The RISE Special Volume presents results deduced from four field studies and two different numerical model applications, including an ecosystem model, on the buoyant plume originating from the Columbia River. This introductory paper provides background information on variability during RISE field efforts as well as a synthesis of results, with particular attention to the questions and hypotheses that motivated this research. RISE studies have shown that the maximum mixing of Columbia River and ocean water occurs primarily near plume liftoff inside the estuary and in the near field of the plume. Most plume nitrate originates from upwelled shelf water, and plume phytoplankton species are typically the same as those found in the adjacent coastal ocean. River-supplied nitrate can help maintain the ecosystem during periods of delayed upwelling. The plume inhibits iron limitation, but nitrate limitation is observed in aging plumes. The plume also has significant effects on rates of primary productivity and growth (higher in new plume water) and microzooplankton grazing (lower in the plume near field and north of the river mouth); macrozooplankton concentration (enhanced at plume fronts); offshelf chlorophyll export; as well as the development of a chlorophyll "shadow zone" off northern Oregon.

Citation: Hickey, B. M., et al. (2010), River Influences on Shelf Ecosystems: Introduction and synthesis, *J. Geophys. Res.*, *115*, C00B17, doi:10.1029/2009JC005452.

1. Introduction: RISE Hypotheses

[2] The coastal waters of the U.S. Pacific Northwest (PNW) house a rich and productive ecosystem. However, chlorophyll is not uniform in this region: it is typically greater in the Columbia River plume and over the coast north of the Columbia river mouth than south of the plume, as illustrated in Figure 1. This view is supported on a seasonal basis by time series of vertically integrated chlorophyll [*Landry et al.*, 1989] and by satellite-derived ocean color [*Strub et al.*, 1990; *Thomas et al.*, 2001; *Legaard and Thomas*, 2006; *Thomas and Weatherbee*, 2006; *Venegas et al.*, 2008]. South of the Columbia river mouth and plume, only over Heceta Bank does chlorophyll approach values as high as over the northern shelves (Figure 1). The higher chlorophyll concentrations of the northern PNW coast are surprising because alongshore wind stress, presumed responsible for macronutrient supply in this Eastern Boundary upwelling system, increases southward over the California Current System (CCS) by a factor of eight [*Hickey and Banas*, 2003, 2008; *Ware and Thomson*, 2005]. Greater productivity off the northern coast and near the Columbia plume has also been reported in higher trophic groups (e.g., euphausiids and copepods) [*Landry and*

[1]School of Oceanography, University of Washington, Seattle, Washington, USA.
[2]Department of Ocean Sciences, University of California, Santa Cruz, California, USA.
[3]College of Ocean and Atmospheric Sciences, Oregon State University, Corvallis, Oregon, USA.
[4]Northwest Fisheries Science Center, NOAA Fisheries, Newport, Oregon, USA.
[5]Department of Civil and Environmental Engineering, Portland State University, Portland, Oregon, USA.
[6]Applied Physics Laboratory, University of Washington, Seattle, Washington, USA.
[7]Science and Technology Center for Coastal Margin Observation and Prediction, Oregon Health and Science University, Beaverton, Oregon, USA.
[8]Department of Civil and Environmental Engineering, University of Washington, Seattle, Washington, USA.
[9]Department of Aviation, University of New South Wales, Sydney, New South Wales, Australia.
[10]Lamont-Doherty Earth Observatory, Earth Institute at Columbia University, Palisades, New York, USA.
[11]SEOS, University of Plymouth, Plymouth, UK.

0148-0227/10/2009JC005452$09.00

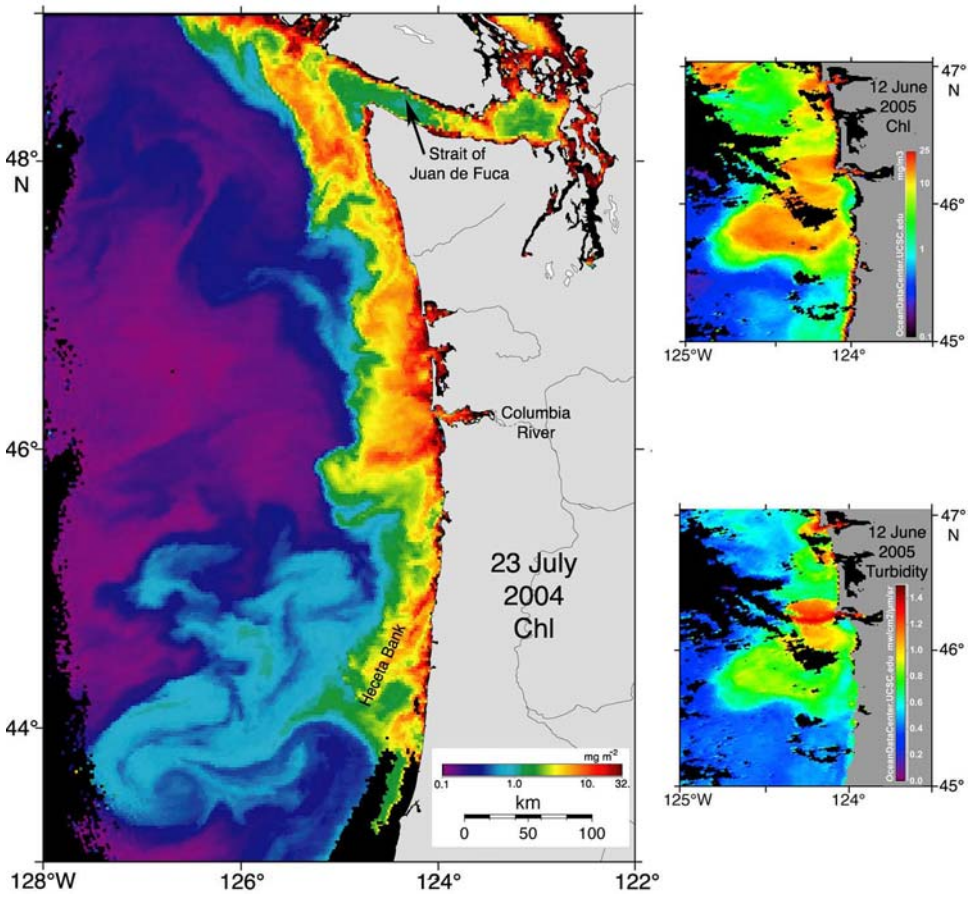

Figure 1. (left) Satellite-derived chlorophyll data (23 July 2004) illustrating the typically observed higher chlorophyll in the Columbia plume as well as north of the river mouth (compared to south of the plume). The image was obtained under strong upwelling conditions, with a well-developed southwest tending plume as well as remnants of a north tending plume [*Liu et al.*, 2009a]. Alongshore chlorophyll patterns agree well with observations presented later in the paper (Figure 7a). (right) Satellite-derived chlorophyll and turbidity 12 June 2005 illustrating a well-developed southwest tending Columbia plume and a weaker north tending plume. The image was obtained one day after model runs shown in Figure 10. Data acquired from Kudela Laboratory.

Lorenzen, 1989]. In spring and summer, juvenile salmon are more abundant on the shelf north of the river mouth [*Pearcy*, 1992; *Bi et al.*, 2007; J. O. Peterson, unpublished data, 2009].

[3] In 2004 an interdisciplinary study "River Influences on Shelf Ecosystems" (RISE) was initiated to determine the extent to which alongshore gradients in ecosystem productivity might be related to the existence of the massive freshwater plume from the Columbia River. RISE was designed to test three hypotheses: (1) During upwelling the growth rate of phytoplankton within the Columbia plume exceeds that in nearby areas outside the plume being fueled by the same upwelling nitrate. (2) The plume enhances cross-margin transport of plankton and nutrients. (3) Plume-specific nutrients (Fe and Si) alter and enhance shelf productivity preferentially north of the river mouth.

[4] RISE is the first comprehensive interdisciplinary study of the rates and dynamics governing the mixing of river and coastal waters in an eastern boundary system, as well as the effects of the buoyant plume formed by those processes on phytoplankton growth and grazing rates, standing stocks and community structure in the local ecosystem. This paper presents an overview of the project measurements and setting as well as a synthetic view of results. Background information on shelf processes, the Columbia River estuary and the Columbia River plume is presented in section 2, followed by a description of the RISE sampling scheme and numerical models (section 3). The environmental and biological setting of the RISE study years is given in section 4. Study results as they pertain to plume-related questions and hypotheses are discussed in section 5 and summarized in section 6.

2. Background

2.1. Shelf Processes Influencing the Columbia Plume

[5] The buoyant plume from the Columbia River is located near the northern terminus of an eastern boundary current. Water property, nutrients, biomass and current variability are governed by wind-driven processes and dominated by the seasonal cycle. The seasonal variability of physical, chemical and biological properties for both

Oregon and Washington are documented in *Landry et al.* [1989] and in the book edited by *Landry and Hickey* [1989]. In winter, large-scale currents are primarily northward (the Davidson Current); in summer, large-scale currents are primarily southward (the California Current) [*Hickey*, 1979, 1989, 1998]. A coast-wide phenomenon that initiates the uplift of isopycnals and associated higher nutrient and lower oxygen water from the continental slope to the shelf, the "Spring Transition" [*Huyer et al.*, 1979; *Strub et al.*, 1987], separates winter from the springtime growing season. Both the spring transition and the seasonal continuation of upwelling through the fall season have been attributed in part to winds south of the region (i.e., "remote forcing") [*Strub et al.*, 1987; *Hickey et al.*, 2006; *Pierce et al.*, 2006]. The uplifted isopycnals result in the formation of a southward baroclinic coastal jet, a feature which in mid summer is generally concentrated over the outer shelf and upper slope off the coasts of northern Oregon [*Kosro*, 2005] and Washington [*MacFadyen et al.*, 2005].

[6] Fluctuations in currents and water properties in this region occur on scales of 2–20 days throughout the year [*Hickey*, 1989]. These fluctuations are driven in part by fluctuations in local winds, and in part by coastally trapped waves generated by remote winds [*Battisti and Hickey*, 1984]. Although, a change in wind direction from upwelling favorable (southward) to downwelling favorable (northward) reverses the direction of flow from southward to northward on the inner shelf where flow is frictionally dominated [*Hickey et al.*, 2005], surface currents on the outer shelf and slope rarely reverse [*Kosro*, 2005; *MacFadyen et al.*, 2008]. The stability of the shelf break jet is due primarily to its baroclinic nature: reversals of wind stress to downwelling favorable are insufficient to completely erode the seasonally uplifted isopycnals during the upwelling season. However, within a distance of about 10 km from the coast (the scale of the internal Rossby radius of deformation), the response to changes in wind direction is almost immediate (~3 h) [*Hickey*, 1989], resulting in significant vertical movement of isopycnals on time scales of a few days. When winds are directed southward, the associated upwelling of nutrient-rich water on the inner shelf fuels coastal productivity, resulting in changes in chlorophyll concentration that follow the changes in wind direction. During an upwelling event, phytoplankton begin to grow as a response to the infusion of nutrients near the coast and this "bloom" is advected offshore, continuing to grow while depleting the nutrient supply. When winds relax or reverse, the bloom moves back toward shore where it can contact the coast and even enter coastal estuaries [*Roegner et al.*, 2002].

[7] Although alongshelf currents do not typically reverse on the mid to outer shelf, currents in the surface Ekman layer frequently reverse from onshore to offshore and vice versa in response to southward or northward wind stress, respectively [*Hickey et al.*, 2005]. Cross-shelf movement of buoyant plumes is particularly sensitive to wind stress direction, because the Ekman layer is compressed by the plume stratification so that velocities are correspondingly higher [*Garcia-Berdeal et al.*, 2002].

[8] Water flowing south toward the Columbia plume region in summer has its source in a topographically complex region offshore of the Strait of Juan de Fuca, which includes a seasonal eddy (Figure 2). Enhanced upwelling, in combination with outflow from the Strait, makes this region a massive source of nutrients and chlorophyll for the shelf north of the Columbia River [*MacFadyen et al.*, 2008]. Upwelled nitrate supplied to this region by Strait related processes is about the same magnitude as that supplied to the entire Washington coast over the upwelling season [*Hickey and Banas*, 2008]. Moreover, the elevated nitrate is distributed to greater distances offshore because of the Juan de Fuca eddy, and to greater depths in the water column because of the Strait outflow, so that this region is particularly rich in chlorophyll [*Hickey and Banas*, 2008]. Water from this region can transit the entire Washington shelf from north to south in a week or less under strong upwelling conditions [*MacFadyen et al.*, 2008].

2.2. Columbia River Estuary

[9] The Columbia estuary has been the subject of a number of physical oceanographic studies [*Hughes and Rattray*, 1980; *Giese and Jay*, 1989; *Hamilton*, 1990; *Jay and Smith*, 1990a, 1990b, 1990c; *Jay and Musiak*, 1996; *Cudaback and Jay*, 2000, 2001; *Kay and Jay*, 2003a, 2003b; *Orton and Jay*, 2005; *Chawla et al.*, 2008]. The width of the estuary at its mouth is about 4 km and the depth over the bar is about 18 m. The ratio of the estuary width at the mouth to the baroclinic Rossby radius near the mouth is typically about 0.2–0.4 (the Kelvin number), so the estuary is considered dynamically narrow. The tidal prism (defined as the integrated volume between mean lower low and high waters) varies from about half to ten times the river flow volume. The density field within the estuary normally alternates between two states: one, weakly stratified or partially mixed, which occurs during low flow periods with strong tides; the other, highly stratified (nearly salt wedge), which occurs under most other conditions. Early interdisciplinary studies on the estuary and plume were summarized in the book by *Pruter and Alverson* [1972]. More recently, the Columbia estuary has been the focus of a Land Margin Ecosystem Research (LMER) program [*Simenstad et al.*, 1990a]. The estuarine ecosystem is supported largely by exogenous organic material supplied by the river, rather than by in situ primary production [*Simenstad et al.*, 1990b; *Sullivan et al.*, 2001; *Small et al.*, 1990]. Export of chlorophyll from the estuary to the plume is minimal, and occurs preferentially on spring tides before and after the spring freshet season [*Fain et al.*, 2001; *Sullivan et al.*, 2001].

2.3. Columbia River Plume

[10] The Columbia River accounts for 77% of the drainage along the U.S. West coast north of San Francisco [*Barnes et al.*, 1972]. The plume from the Columbia varies in volume from 2 to 11 $\times$ 10^{10} m^3, with maximum volume due to late spring snowmelt freshets and in winter due to rainfall [*Hickey et al.*, 1998] and a seasonal minimum in late summer/early fall. Riverflow into the estuary varies from about 2.5–11 $\times$ 10^3 m^3 s^{-1} over a typical year [*Bottom et al.*, 2005]. Summertime river input into the other two coastal estuaries off the Washington coast is typically less than 1% of that from the Columbia River [*Hickey and Banas*, 2003]. The Columbia River plume is more strongly forced at the estuary boundary than other U.S. river systems, creating a spatially and temporally complex region

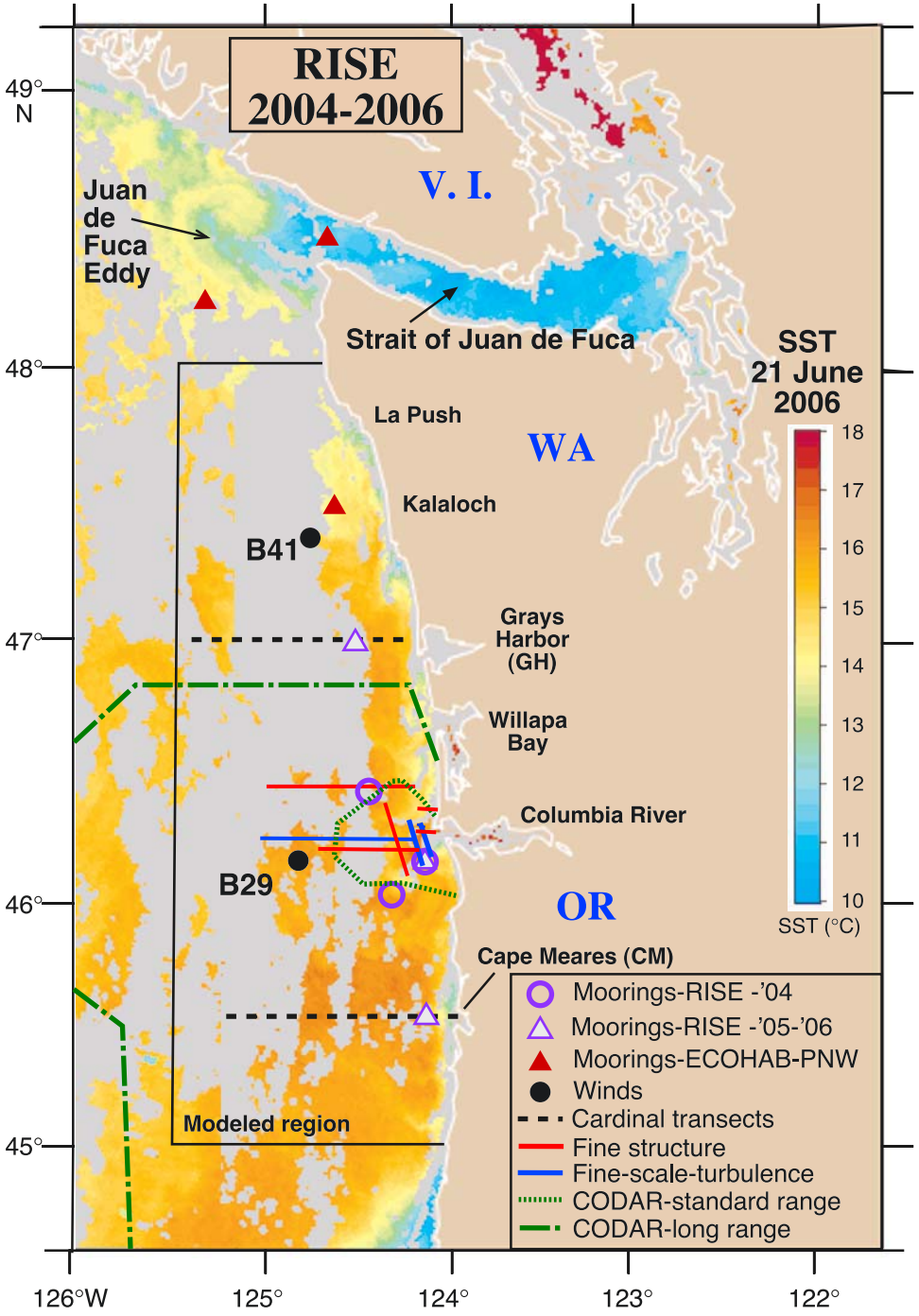

Figure 2. Locations of all sampling transects, moored sensor arrays and wind buoys, and CODAR ranges plotted on a satellite-derived sea surface temperature image on 21 June 2006. Regional physical features of interest are noted.

near the river mouth. Because of the narrow outlet to the ocean, strong tidal currents and significant freshwater flow, surface currents in the tidal plume often exceed 3 m s^{-1} during strong ebb tides. As a result the Columbia River produces a highly supercritical outflow that propagates seaward as a gravity current during each ebb tide. The leading edge front, termed the "tidal plume front," produces strong horizontal convergences, vertical velocities and mixing [*Orton and Jay*, 2005; *Morgan et al.*, 2005].

[11] The historical picture of the Columbia River plume depicts a low salinity feature oriented southwest offshore of the Oregon shelf in summer (e.g., Figure 1) and north or northwest along the Washington shelf in winter [*Barnes et al.*, 1972; *Landry et al.*, 1989]. The RISE hypotheses were based on that view of the Columbia. Recently, *Hickey et al.* [2005] have demonstrated that the plume can be present more than a hundred kilometers north of the river mouth on the Washington shelf from spring to fall. This study showed that the plume is frequently bidirectional, with simultaneous

branches both north and south of the river mouth. This spatial structure was subsequently confirmed by remote sensing [*Thomas and Weatherbee*, 2006]. During downwelling favorable winds, the southwest plume moves onshore over the Oregon shelf. At the same time, a new plume forms north of the river mouth, trapped within ~20–30 km of the coast. This plume propagates and also is advected northward by inner shelf currents that reverse during the downwelling winds. When winds return to upwelling favorable, inner shelf currents reverse immediately to southward and the shallow plume is advected offshore in the wind-driven Ekman layer to the central shelf, and southward in the seasonal mean ambient flow [*Hickey et al.*, 2005]. The possibility of a bidirectional Columbia plume depends critically on the existence of mean ambient flow in the direction opposite to its rotational tendency. Because three out of four RISE cruises occurred early in the upwelling season, most sampling took place in a bidirectional plume environment.

[12] On subtidal time scales, numerical and laboratory models of river plume formation in a rotating system under conditions of no applied winds and no ambient flow demonstrate that a plume forms a non linear "bulge region" and a quasi-geostrophic "coastal current" downstream of the bulge [e.g., *Chao and Boicourt*, 1986; *Garvine*, 1999; *Yankovsky et al.*, 2001; *Fong and Geyer*, 2002; *Horner-Devine et al.*, 2006]. These prior studies addressed the dynamics of unidirectional plumes for conditions most typical of the U.S. east coast: shallow broad shelves and modest riverflow and ambient flow (if included) in the direction of plume formation. However, the Columbia River generates a large volume plume which emerges onto a relatively narrow continental shelf. Perhaps its most unusual characteristic is that in summer it usually encounters ambient flow moving counter to the rotational tendency of the plume. Prior to RISE, only the model study by *Garcia-Berdeal et al.* [2002] directly addressed conditions applicable to the Columbia. That study provided a dynamical basis for the existence of a bidirectional plume and the time varying response of the plume to variable winds as well as to ambient flow both in the same direction as, and counter to, the rotational tendency. The study also demonstrated that over the shelf away from the river mouth, the effect of the plume on the velocity field is confined to layers of low salinity (i.e., the plume effect is baroclinic), as shown in a wintertime Columbia plume data set [*Hickey et al.*, 1998].

[13] With respect to nutrients, historical studies showed that in summer the Columbia plume usually supplies exceptionally high concentrations of silicic acid but very little nitrate, to the plume region [*Conomos et al.*, 1972]. Because sediment transport and deposition from the Columbia plume is highest north of the river mouth [*Nittrouer*, 1978], that shelf potentially has a massive supply of Fe-rich sediment deposited on the mid shelf region ready to be delivered to the euphotic zone by upwelling of bottom water that has been in contact with the sediments. In addition, the broader, flatter shelf north of the river mouth has been hypothesized to provide opportunity for increased duration of bottom contact (hence access to Fe) of upwelling waters than the narrower, steeper shelf to the south [*Bruland et al.*, 2001; *Chase et al.*, 2007]. The midshelf mud deposits can be thought to act like an iron capacitor; charging in the winter with the higher sediment transport associated with winter flood events, and discharging during the summer upwelling periods.

3. RISE Sampling Scheme and Modeling Systems

[14] The overall RISE sampling strategy was to compare mixing rates, nutrient supply, and phytoplankton production, grazing and community structure within the plume and outside the plume; i.e., on the shelf north of the river mouth, presumed more productive, and on the shelf south of the river mouth, presumed less productive, as well as in the important "plume liftoff" zone (the region where the plume loses contact with the bottom, located in the river entrance to ~5 km offshore of the entrance jetties). The backbone for this project consists of data collected during four cruises that took place in the seasonally high flow period (May–June) in each of three years (2004–2006) and in a low flow period in one year (August 2005). The sampling was spread over three years to include potential interannual differences in processes related to wind and river flow variability. The 21 day length of the cruises ensured that a variety of circulation and growth regimes, including upwelling, relaxation, downwelling, and neap/spring tides were observed. A list of program elements including data collected, models and techniques as well as team leaders is given in Table 1.

[15] The sampling plan as originally proposed was based on the historical picture of a primarily southwest tending Columbia plume. However, due to the rarity of persistent upwelling favorable winds on RISE cruises, southwest tending plumes were the exception rather than the rule. In particular, on two of the cruises, June 2005 and May–June 2006, north tending plumes were dominant: RISE sampling was adapted to this situation, and samples were obtained along the Washington coast as far north as the Strait of Juan de Fuca in 2006.

[16] The field studies used two vessels operating simultaneously. The R/V Wecoma obtained primarily biological and chemical rate data: (1) at individual stations on cardinal transects north and south of the river mouth (Grays Harbor and Cape Meares; see Figure 2) and near the river mouth; (2) at selected process study stations; and (3) at fixed stations near the river mouth during strong neap and spring tides (time series). A towed sensor package was used to obtain micronutrient samples near the sea surface on cardinal transects and selected other transects. Underway measurements included macronutrients (N, P, Si), dissolved trace metals (Fe, Mn), supplemented with discrete samples from the underway system (microscopy, FlowCAM and particulate trace metals) as well as ADCP (75 kHz) measurements of velocity. At CTD stations vertical profiles (0–200 m where possible; and 500 m at selected stations) of T, S, currents, dissolved O_2, in vivo fluorescence, transmissivity, PAR, and bottle samples for chlorophyll *a*, dissolved macronutrients (NO_3, NH_4, urea, PO_4, SiO_4), dissolved trace metals, and heterotrophic and autotrophic plankton composition were obtained. In addition, primary production measurements were made each day at noon, and phytoplankton growth and microzooplankton grazing measurements were made every one to two days. Macrozooplankton were sampled with vertically towed nets and obliquely towed Bongo nets at selected stations; macrozooplankton

Table 1. RISE Program Elements

Component	Techniques	Team Leaders
Management and Synthesis		Hickey
Physical Modeling	Numerical models, ROMS and SELFE with MM5 forcing, NCOM boundaries, tides	MacCready, Baptista
Biophysical Modeling	3D Numerical models	Banas
Water Properties, Underway and CTD	Underway and CTD	Hickey, Jay, Kudela
Water Properties	TRIAXUS tow-fish	Jay
Water Properties	Moored arrays	Dever
Suspended Particulates, Concentration and Size	LISST-FLOC, acoustic backscatter	Jay, Horner-Devine
Chlorophyll *a* and Phaeopigments	In vivo and in vitro fluorometry	Kudela
Dissolved Nutrients including Trace Metals	Surveys and towed fish, Lachat autoanalyzer flow injection, voltammetry, extraction/ICP-MS	Bruland, Kudela
Picoplankton	Flow cytometry	Kudela
Autotrophic/Heterotrophic Pico-, Nano-, Microplankton Abundance/Taxa	Epifluorescence and light microscopy	Lessard
Nitrogen Uptake	^{15}N nitrogen kinetics	Kudela
Phytoplankton Growth and Microzooplankton Grazing Rates	Dilution method – size-fractionated chlorophyll *a*, microscopy	Lessard
Primary Production	^{14}C uptake	Kudela
Macrozooplankton Species and Abundance, Growth, Egg Production	Net tows, Laser Optical Plankton Counter (LOPC), microscopy	Peterson
Hydrology	USGS data	Jay
Water Column Currents	Moorings, ADCP surveys	Dever, Jay
Mixing Rates, Vertical Fluxes	Profiles	Nash, Moum
Surface Eulerian Currents	CODAR, up to 180 km	Kosro
Surface Lagrangian Currents	GPS drifters (with C, T)	Hickey
Remote Sensing of Sea Surface Temperature, Color and Fluorescence	AVHRR, SeaWiFS, MODIS, Bio-Optical modeling	Kudela
Plume Position, Fronts, and Internal Waves	Synthetic Aperture Radar (SAR)	Jay

experimental work included egg production rates of copepods and euphausiids and molting rates of euphausiids, to obtain estimates of secondary production. Surface drifters were used to follow the mixing of individual plumes from the Columbia and to provide information on surface currents.

[17] On the R/V Point Sur, synoptic mesoscale and fine-scale features were sampled with underway measurements of near-surface T, S, velocity, particle size and concentration, PAR, transmissivity, fluorescence, and nitrate + nitrite. The Point Sur's Triaxus tow fish provided high-resolution sections of T, S, zooplankton (Laser-OPC), PAR and transmissivity, fluorescence, particle size and concentration (LISST-100), UV absorption and nitrate (Satlantic ISUS), upward-looking ADCP velocity (1200 kHz), and radiance/irradiance (7 channels) through the upper water column to 30–35 m. Rapidly executed transects of turbulence and fine structure were also carried out using the Chameleon profiler; these provide full depth profiles of T, S, optics (880 nm backscatter and fluorescence), turbulence dissipation rates and fluxes every 1–3 min. During selected periods, transects (primarily those identified in Figure 2) were repeated hourly to capture the high-frequency evolution in the plume's near-field and river estuary. Over-the-side deployed acoustics (1200 kHz ADCP and 120 kHz echosounder; 1 m nominal depth) augmented the hull-mounted 75 and 300 kHz units to image fine-scale features of the velocity and backscatter fields, resolving fronts, nonlinear internal waves, and turbulent billows.

[18] The temporal context for observed variability was provided by an array of moored sensors deployed in the plume near field as well as on the shelf north and south of the plume (Figure 2), complemented by the preexisting long-term estuarine and plume stations of the CORIE/SATURN network [*Baptista*, 2006]. To better resolve regional differences, RISE moorings were moved farther north and south to the cardinal sampling transects after the first year of the program (Figure 2). Surface currents were mapped hourly from shore using HF radar with two simultaneously operating arrays, one with a 40 km range and a 2 km range resolution, the other with a 150 km range and a 6 km range resolution. Satellite ocean color, sea surface temperature, turbidity and synthetic aperture radar (SAR) were also obtained when available.

[19] Two modeling systems were developed or enhanced during RISE. The system developed specifically for RISE employed a structured grid model (the Regional Ocean Modeling System (ROMS)) and was used in hindcast mode [*MacCready et al.*, 2009]. The CORIE/SATURN modeling system [*Baptista*, 2006], based on two unstructured grid models (SELFE, *Zhang and Baptista* [2008]; ELCIRC, *Zhang et al.* [2004]), was used in both near real-time prognostic mode (http://www.stccmop.org/datamart/forecasts/simpletool) and multiyear hindcast mode [e.g., *Burla et al.*, 2009]. Both modeling systems incorporated the estuary in the simulation domain (although at different resolutions) and used realistic atmospheric, river and ocean forcing including tides. Wind/heat flux model forcing for ROMS was derived from the 4 km MM5 regional wind/heat flux model [*Mass et al.*, 2003]. SELFE and ELCIRC were also forced by MM5. Conditions on open boundaries were provided by Naval Research Laboratory (NRL) models; ROMS used the smaller domain, higher-resolution (~9 km) NCOM-CCS NRL model [*Shulman et al.*, 2004], SELFE and ELCIRC used the larger domain, lower-resolution (~16 km) global NCOM model [*Barron et al.*, 2006]. These models have proven more effective in this region than climatology because they assimilate satellite altimetry and sea surface temperature,

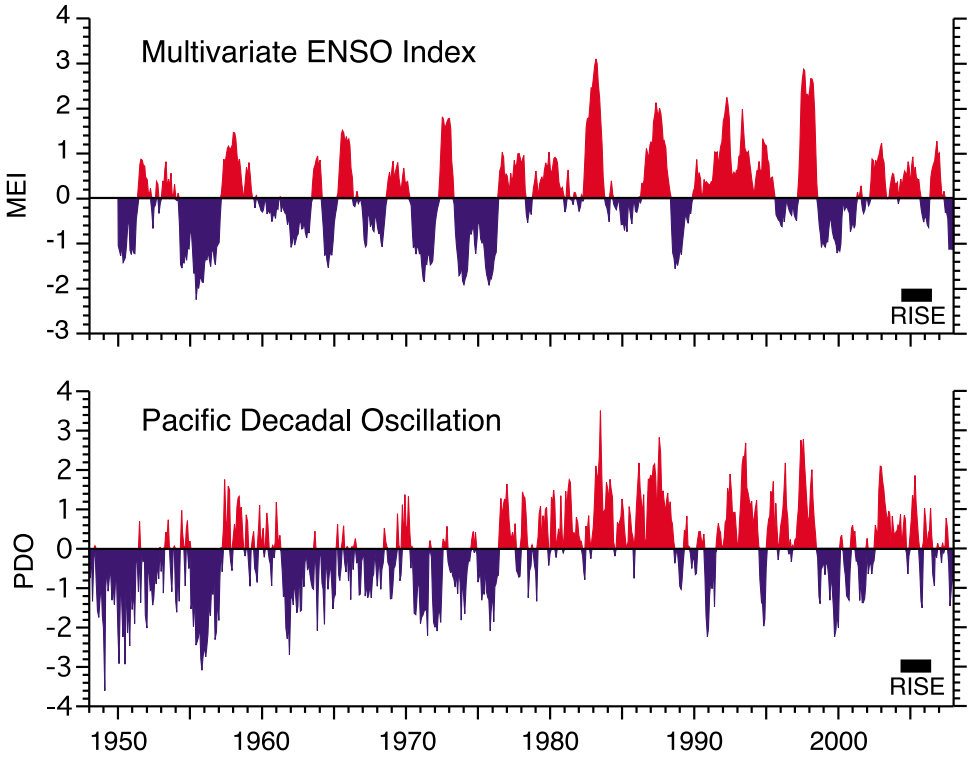

Figure 3. The Multivariate ENSO Index (MEI) and the Pacific Decadal Oscillation Index (PDO) from 1950 to the present. The MEI is computed from the six main observed variables in the tropical Pacific [*Wolter and Timlin*, 1993]. The PDO is defined as the leading principal component of North Pacific monthly sea surface temperature variability (poleward of 20°N for the 1900–1993 period) [*Mantua et al.*, 1997].

thus ensuring the reasonable development of a southward coastal jet, as well as inclusion of low mode coastal trapped waves that are a significant part of the subtidal scale variance at midshelf in this region [*Battisti and Hickey*, 1984]. Both models became integral tools for planning and/or analysis within RISE.

[20] The ROMS model was also used for biologically motivated particle-tracking studies [*Banas et al.*, 2009a] and ecosystem modeling [*Banas et al.*, 2009b]. The biological model is a four-box ("NPZD") nitrogen budget model that tracks nutrients, phytoplankton, microzooplankton, and detritus in every cell of the ROMS grid. The rich RISE biological data set allowed direct model validation against not just stocks (chlorophyll, microzooplankton, nutrients) but rates (phytoplankton growth and microzooplankton grazing), a level of validation that is seldom possible. Rate observations also allowed key model parameters (e.g., microzooplankton ingestion rate and mortality) to be prescribed empirically [*Banas et al.*, 2009b].

[21] During the RISE field years, another interdisciplinary program took place along the central to northern Washington, southern British Columbia coast. This project (Ecology of Harmful Algal Blooms Pacific Northwest, ECOHAB PNW), with a scientific team and suite of measurements similar to that of RISE, focused on the development of blooms of toxigenic *Pseudo-nitzschia* in the Juan de Fuca eddy region (see Figure 2) and their subsequent transport to the Washington coast. Surveys were made as far south as offshore of Willapa Bay, and as far north as central Vancouver Island. Both RISE and ECOHAB PNW sampled a line off Grays Harbor, and the combined survey data were used in several papers in this and previous volumes [*Hickey et al.*, 2006; *Kudela et al.*, 2006; *Frame and Lessard*, 2009]. Data from the moored arrays in the two programs (see locations in Figure 2) have also been used together in papers for this volume [*Hickey et al.*, 2009].

4. The RISE Years: Environmental and Biological Setting

[22] Time series of the two commonly used indices for interannual variability, the Multivariate El Niño/Southern Oscillation Index (MEI) and the Pacific Decadal Oscillation (PDO) illustrate that RISE studies all took place within periods when both indices were generally positive (Figure 3). Columbia and Willamette River (a major lower basin Columbia River tributary) flows are lowest in years when the PDO is positive (with a warm coastal ocean in the Pacific Northwest) and the MEI index is positive (indicating El Niño-like conditions). Average flows are about 20% lower than in La Niña years when the PDO is negative [*Dracup and Kahya*, 1994; *Gershunov et al.*, 1999; *Bottom et al.*, 2005]. Indeed, riverflow was below average in spring of all RISE years except during a brief period in late May 2005 and from April though June 2006 (Figure 4a). In May 2005, flow in the Willamette River was unusually high (up to 200% of normal), leading to above average export of nutrients from the estuary to the plume. Compared to

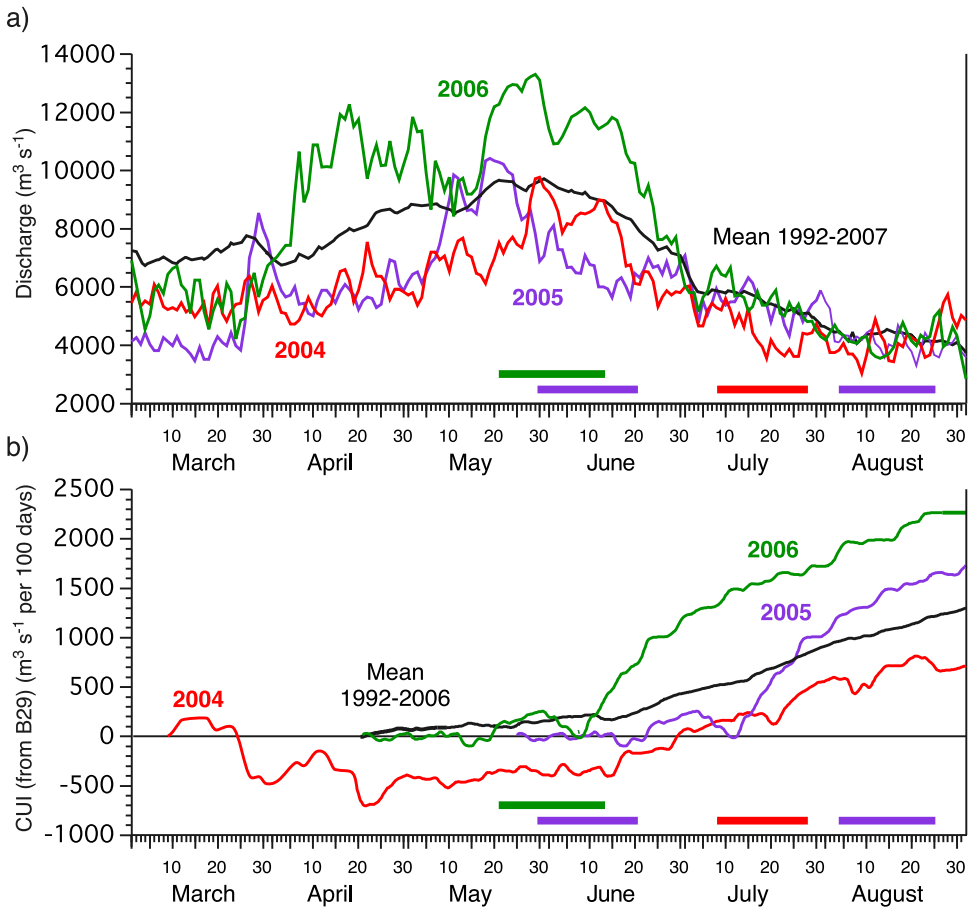

Figure 4. (a) Seasonal Columbia River discharge measured at Beaver Army terminal for 2004, 2005, and 2006, along with average discharge 1992–2007. RISE field studies are indicated with the colored bars parallel to the *x* axis. (b) Cumulative upwelling index (CUI) [*Bakun*, 1973] calculated from winds at NDBC Buoy 46029 for the upwelling seasons of 2004, 2005, and 2006, along with the average CUI 1992–2007. The location of the wind station is shown in Figure 2. RISE field studies are indicated with the colored bars parallel to the *x* axis. The integration was started at the spring transition each year as defined by M. Kosro (personal communication, 2009).

historical records, nitrate was about a factor of two higher in spring of both 2005 and 2006 in the Columbia River outflow, in large part due to additional nutrient sources from coastal and valley rivers, in particular, those that had been recently logged [*Bruland et al.*, 2008].

[23] Warmer than average surface waters were observed in the Pacific Northwest during the RISE summers [*Shaw et al.*, 2009], consistent with the occurrence of positive phases of MEI and PDO. The fact that the warmer water is related to advection rather than local heating is confirmed with time series of copepod species assemblages (Figure 5). In an average year, during winter months the northward flowing Davidson Current transports warm water "neritic" species (species restricted to coastal shelf environments) northward from California to the Oregon and Washington shelves; during the upwelling season, cold water species usually dominate and these species are transported southward from coastal British Columbia and the coastal Gulf of Alaska. During the RISE project summers of 2003 through 2005 the copepod community was dominated by "warm water neritic" species, as typically occurs when the PDO is positive [*Hooff and Peterson*, 2006]. The community began to transition to a cold water species phase during the summer of 2006, consistent with the decreasing PDO (Figure 3); however "warm water oceanic" species were still conspicuous in samples. Figure 3 also shows that during strong El Niño events (as in late 1997–1998) the copepod community is also dominated entirely by warm water species (for both neritic and oceanic species). Thus, the RISE years were similar in some respects [biological (zooplankton) and physical (riverflow and surface water temperatures)] to El Niño conditions.

[24] In spite of the low overall riverflow and El Niño-like conditions, short-term variability in physical and biological conditions in this region is sufficiently strong that conditions of both high and low riverflow, upwelling and downwelling occurred and were sampled during the RISE cruises. The RISE 1 cruise in July 2004 took place in a year with the lowest July riverflow observed during RISE years (Figure 4a). The cruise included a period of persistent upwelling winds and, perhaps more significant, the largest southward flows sampled during the RISE cruises (Figure 6). A well-developed southwest tending plume was observed, and samples were taken along its axis. Nitrate was supplied

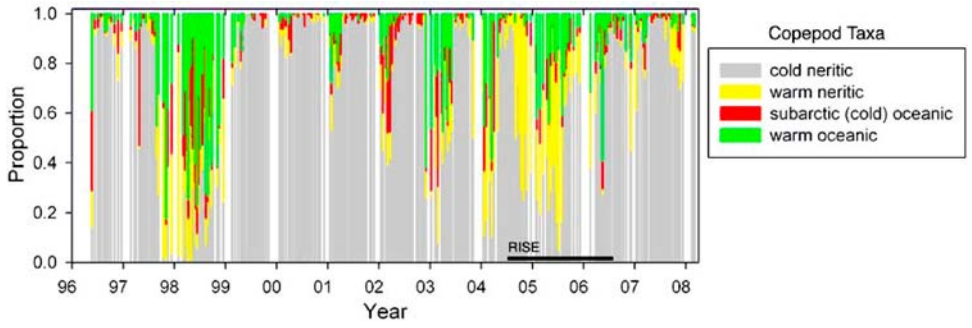

Figure 5. Proportion of copepod community types in zooplankton tows at a station 9 km offshore on the Newport line (44°39.1′N, 124°10.6′W). The length of each color bar is proportional to the amount of that taxa. Data acquired from Peterson Lab.

to the plume via upwelled nitrate-rich waters mixing with nitrate-depleted river water during plume formation [*Bruland et al.*, 2008]. Seasonal upwelling favorable winds prior to the cruise were the weakest observed during RISE years (Figure 4b).

[25] In 2005, upwelling over the inner shelf was delayed [*Hickey et al.*, 2006; *Kosro et al.*, 2006] and the May–June RISE 2 cruise took place prior to the onset of strong upwelling favorable winds and just after a period of higher than average riverflow (Figures 4a and 6). A weak southwest tending plume was observed at the beginning of the cruise, but most cruise sampling took place in a northward tending plume. Plume nutrients were being supplied from the watershed rather than from the coastal ocean [*Bruland et al.*, 2008],

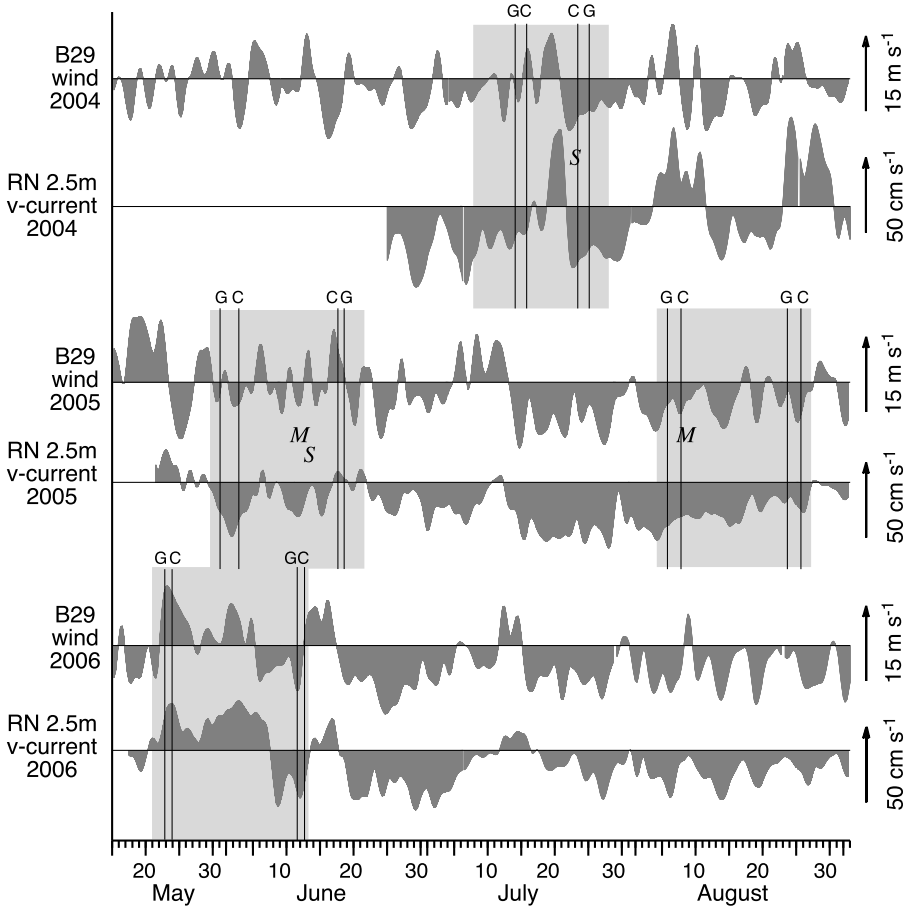

Figure 6. Alongshelf component (positive northward) of wind at Buoy 46029 and near-surface current at mooring RN, north of the Columbia mouth (see location in Figure 2) for each of the RISE field seasons. The shipboard field studies are shown with shaded bars. Sections from the ''cardinal'' sampling transects offshore of Grays Harbor (G) and Cape Meares (C) are indicated with vertical lines. Satellite data used in this paper (Figure 1) are indicated (S) along with times of model runs displayed in Figure 10 (M). Current data provided by Dever Lab.

resulting in substantially lower than expected coastal productivity [*Kudela et al.*, 2006].

[26] RISE 3 took place in August 2005 in a period with the lowest riverflow of all the RISE cruises (Figure 4a) and after upwelling favorable winds had become persistent (Figures 4b and 6). A strong well-developed southwest plume was observed and sampled. This was the only observation of actual upwelling off the Washington coast in all of the RISE cruises. Plume nutrients were being provided from upwelling water that mixed with the outflowing riverflow [*Bruland et al.*, 2008].

[27] The final RISE cruise took place in May–early June 2006 under extremely high riverflow conditions, the highest observed in the four RISE cruises (Figure 4a). Downwelling favorable winds were also higher than typically observed at that time of year as indicated by the significant dip in the cumulative wind stress curve during the cruise period (Figures 4b and 6). The majority of the cruise time was used sampling north tending plumes, following the plumes as far north as the Strait of Juan de Fuca [*Hickey et al.*, 2009]. However, a new southwest tending plume developed during the last few days of the cruise. In that period, the river itself was supplying plume nutrients to both north and southwest tending plumes [*Bruland et al.*, 2008]. Surface drifters were used to follow the newly emerging southwest plume, sampling its chemical and biological aging with cross-plume transects [*Hickey et al.*, 2009].

5. RISE Results

[28] Several key issues on the development, evolution and importance of river plumes to the regional ecosystem remained at the outset of RISE. One of the least understood phenomena with respect to river plumes was how the freshwater discharge mixes with ambient coastal waters [*Boicourt et al.*, 1998; *Wiseman and Garvine*, 1995]. Another important issue was the effect of a buoyant plume on local transport pathways. A third critical issue was captured by the overall RISE question: how does a buoyant plume impact the ecosystem? The results of RISE as they pertain to these important issues, as well as our ability to model these processes and impacts are summarized below.

5.1. Regional Plume Effects

5.1.1. Does the Plume Alter Phytoplankton Growth Rates, Grazing Rates, or Species Composition in Comparison to Active Upwelling Regions?

[29] A trend toward higher biomass of phytoplankton on the Washington versus Oregon shelf has been attributed to increased retention due to shelf width and/or intermittency or duration of wind forcing, as well as effects of freshwater [*Hickey and Banas*, 2003, 2008; *Ware and Thomson*, 2005], enhanced nitrate supply [*Hickey and Banas*, 2008] and iron availability [*Lohan and Bruland*, 2006; *Chase et al.*, 2007]. Chlorophyll data taken on near-simultaneous RISE sections off Washington and central Oregon are consistent with this pattern (Figure 7a): chlorophyll concentrations are almost always higher toward the north. Chlorophyll data from selected biological process stations averaged over each 21 day cruise are also consistent with the general trend of higher chlorophyll to the north, although the difference is not significant [*Frame and Lessard*, 2009]. The data in Figure 7a were derived from regression between CTD fluorescence and measured chlorophyll ($r^2 \sim 0.72-0.77$ for the four cruises). However, even isolated extrema such as on 22 May 2006 on the GH transect were very similar to the bottle-derived surface Chl values. Surface concentrations were higher to the south at stations close to the coast in the two periods when upwelling was occurring (July 2004 and August 2005), consistent with the tendency for stronger and earlier upwelling off Oregon. The surface cross shelf chlorophyll structure along the GH and CM transects on 23–25 July 2004 in Figure 7a is very similar to that shown in the satellite image of 23 July 2004 (Figure 1): the higher surface chlorophyll extending across much of the shelf off Grays Harbor is reflective of the higher surface chlorophyll along most of the Washington/southern British Columbia coast. This feature terminates south of the Columbia plume region and consequently is not observed off Cape Meares.

[30] In RISE, we addressed the role of the Columbia River plume on phytoplankton growth, grazing and physiology using a number of empirical and modeling approaches. We directly compared phytoplankton intrinsic growth and grazing rates [*Lessard and Frame*, 2008; E. J. Lessard et al., Patterns and control of phytoplankton growth, grazing and chlorophyll on the northeast Pacific coast, manuscript in preparation, 2009] in over 100 dilution experiments as well as plankton community composition [*Frame and Lessard*, 2009] within the plume and on the Washington and Oregon shelves. Phytoplankton intrinsic growth rates were not different on the Washington and Oregon shelves, but were significantly higher in the near-field Columbia plume region. Grazing pressure (grazing:growth ratio) was lowest in the near-field plume and highest off Oregon [*Frame and Lessard*, 2009].

[31] Diatoms dominated the phytoplankton biomass in most samples, and diatom community composition was very similar on both shelves within a cruise; there was no strong evidence for a unique phytoplankton assemblage within the plume [*Frame and Lessard*, 2009]. Nevertheless, when assemblages inside and outside plumes were compared for individual plume events, differences in community composition were sometimes observed. For example, samples closely spaced in time during a southwest plume event in August 2005 and also a north plume event in spring 2006 had different nondiatom communities in the plume and outside the plume; and a southwest plume in spring 2006 had different diatom communities inside and outside the plume [*Frame and Lessard*, 2009].

[32] Phytoplankton net growth and chlorophyll size fractions were examined in a series of multiday deckboard incubations with added nutrients or filtered plume water in summer 2005 [*Kudela and Peterson*, 2009]. There was no evidence for an inherent physiological difference in phytoplankton assemblages between the Oregon and Washington shelf waters adjacent to the Columbia River plume, nor was there evidence for short-term effects of iron limitation or enhancement by other constituents of the plume water (e.g., Zn, organic matter). However, *Frame and Lessard* [2009] noted that in spring 2006, after an earlier strong upwelling event and intense diatom bloom, the coastal water outside the plume had residual nitrate and was dominated by small cells (cyanobacteria and picoeukaryotes), consistent with possible iron limitation at that time.

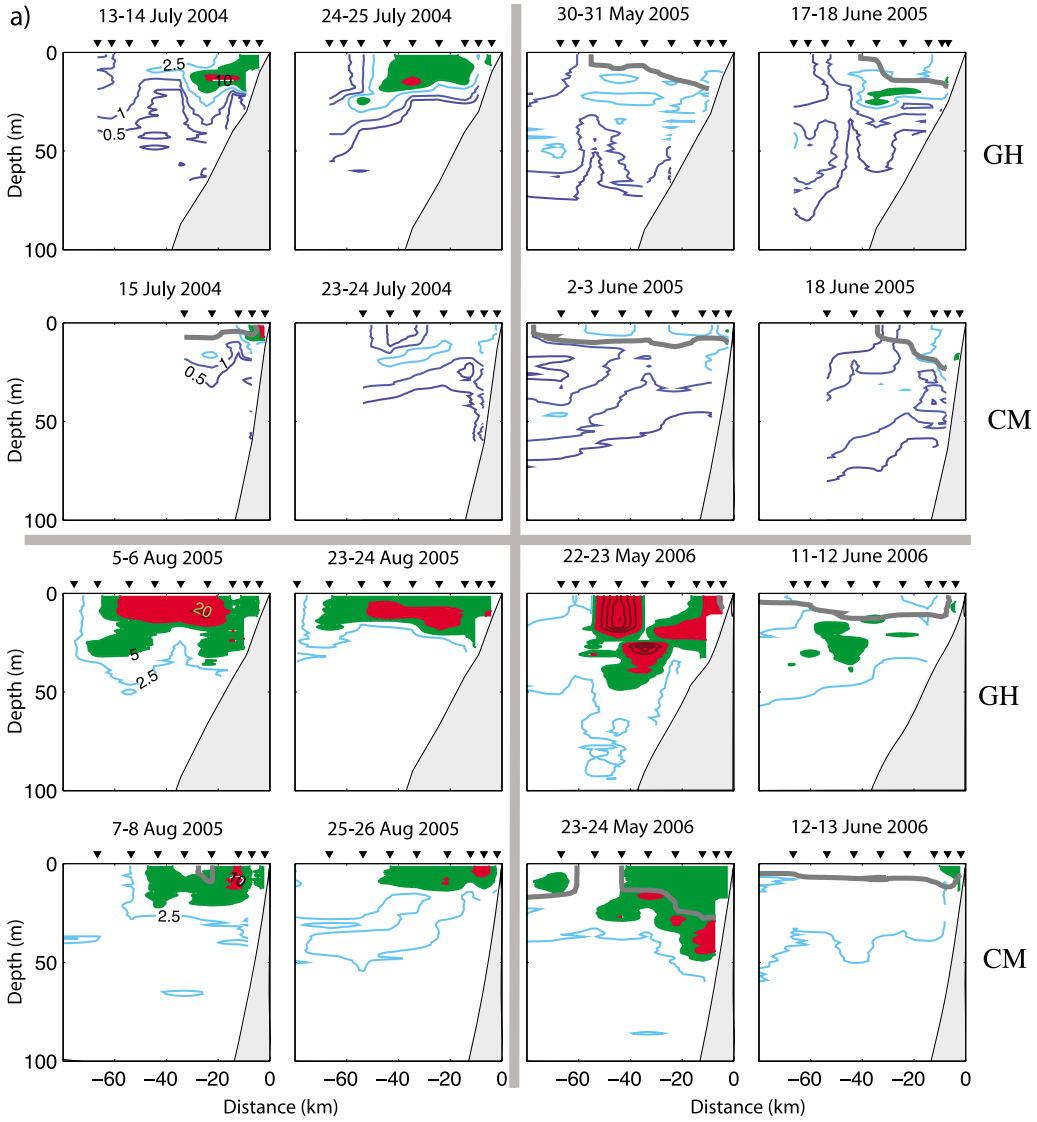

Figure 7. Contoured sections of (a) chlorophyll in mg L^{-1} and (b) nitrate in μM along the RISE cardinal transects ~100 km north (GH) and south (CM) of the Columbia River mouth, illustrating alongshore similarities and differences between the central Washington and northern Oregon coasts. The gray vertical and horizontal bars group the sections from the 4 cruises. In each cruise, the sections were sampled within 1–2 days of each other at the beginning and again at the end of the cruise. Stations are indicated with inverted triangles; bottle samples (nitrate only) are indicated with dots. Environmental settings are shown in Figure 6 and the location of the Columbia River plume is indicated with the heavy gray contours (S<31 psu above the contour). Chlorophyll values above 5 and above 10 mg L^{-1} are indicated with green and red shading, respectively; nitrate values below 1 μM and between 25 and 30 μM are shaded blue and red, respectively. Data from Bruland (nitrate) and Kudela (fluorescence to chlorophyll regression).

[33] The alongshore difference in grazing pressure (higher off Oregon than off Washington) likely plays a significant role in maintaining higher chlorophyll concentrations on the Washington shelf [*Lessard and Frame*, 2008; Lessard et al., manuscript in preparation, 2009]. In addition, model results show that the plume forms a "barrier" to biomass transport to Oregon, deflecting up to 20% of the phytoplankton biomass offshore (see below) [*Banas et al.*, 2009b]. The wider shelf north of the Columbia (affecting retention patterns and possible bloom spin-up times) as well as the retentive characteristics of the Juan de Fuca eddy that feeds the Washington shelf from the north also play important roles in producing alongcoast spatial gradients in chlorophyll [*Hickey and Banas*, 2008].

[34] Historical data suggest that the abundance of macrozooplankton such as copepods and euphausiids is higher off the Washington coast (north of the Columbia River entrance) than south of it (net tow data, *Landry and Lorenzen* [1989]; acoustic data, *Swartzman and Hickey* [2003]). *Swartzman* [2001] shows higher abundances over Washington canyons, leading to the commonly expounded idea that the higher abundances are related to the greater

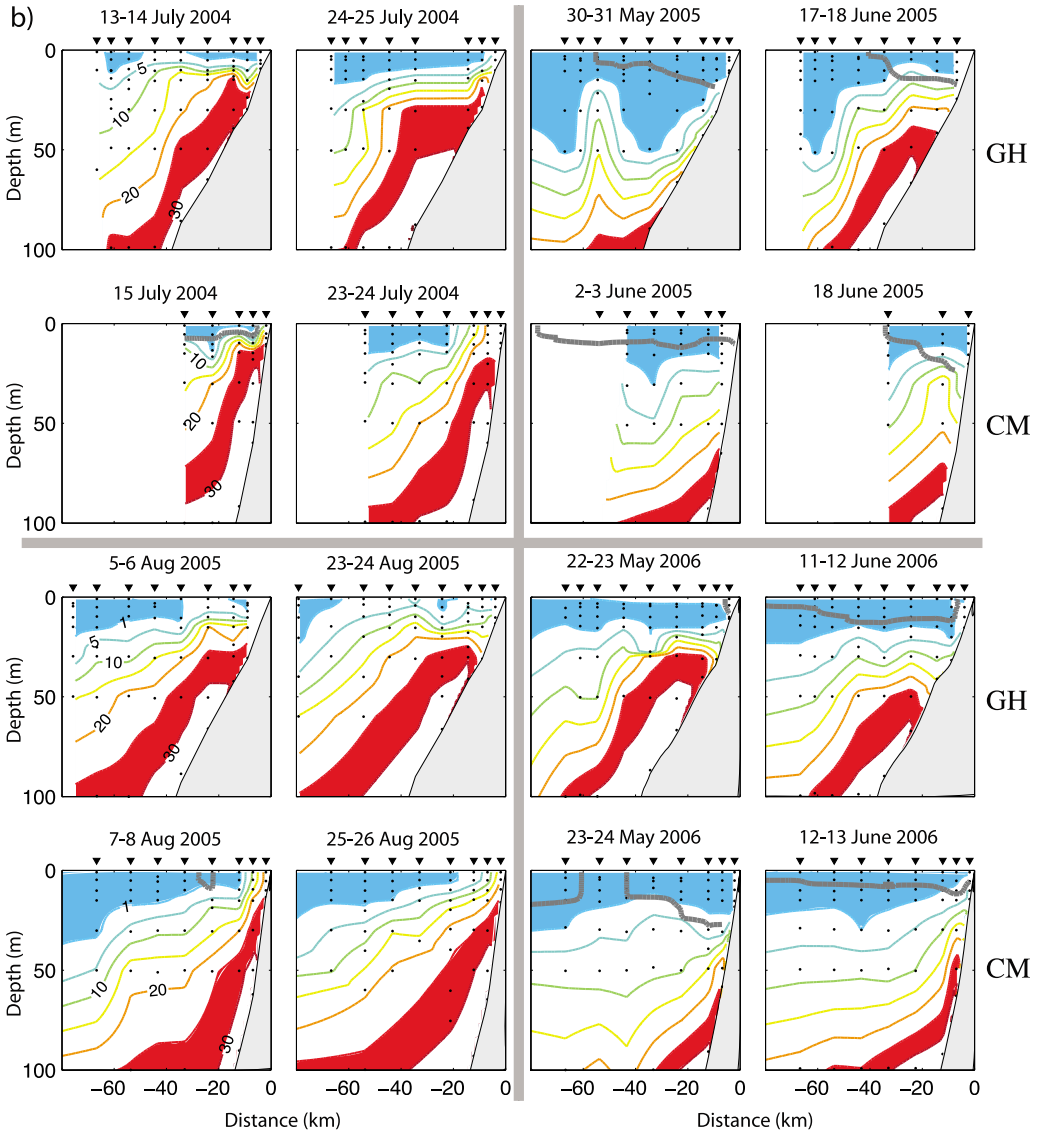

Figure 7. (continued)

number of canyons off Washington. RISE investigators studied egg production and molting rates of two copepod species (*Calanus marshallae* and *C. pacificus*) and two euphausiid species (*Euphausia pacifica* and *Thysanoessa spinifera*) on the shelves north and south of the Columbia River entrance as proxies for adult abundance [*Shaw et al.*, 2009]. *E. pacifica* growth rates were significantly higher during June 2006 than in July 2004 and June 2005, but were not significantly different between the RISE study area and stations off Newport, Oregon. Euphausiid brood sizes were significantly higher during August 2005 than in any of the other cruises for both *E. pacifica* and *Thysanoessa spinifera*, but again there was no indication that brood sizes were higher in the northern part of the RISE study region. Significant differences in egg production rates (EPRs) were found among cruises for both *Calanus pacificus* and *C. marshallae*, with higher EPRs during August 2005, the only cruise with substantial amounts of upwelling. EPRs were low on other cruises, less than half the maximum rates known for these species. Overall, no north–south difference in growth rates was observed, in spite of the suggested north–south differences in adult copepod and euphausiid populations.

5.1.2. Does the Plume Enhance Either Export or Retention of Regional Biomass on the Shelf?

[35] Particle-tracking analysis using the *MacCready et al.* [2009] circulation model demonstrates that the plume disperses water in multiple directions under variable winds [*Banas et al.*, 2009a]. Washington coastal water moves farther north under northward winds when the plume is included in the model, compared with a model scenario in which it is omitted; during some transient conditions coastal water is advected farther south under southward winds as well; and, most significant, coastal water is episodically shifted seaward by plume effects. The mechanisms are a combination of increased entrainment into transient topographic eddies driven by wind intermittency, creation of additional eddies through tidal pulsing [*Horner-Devine et al.*, 2009], shear between the anticyclonic bulge circulation [*Horner-Devine*, 2009] and ambient southward flow [*Yankovsky et al.*, 2001; *Garcia-Berdeal et al.*, 2002], and enhanced offshore flow in the surface Ekman layer of the

plume, which is vertically compressed by the plume stratification [*Garcia-Berdeal et al.*, 2002]. The net effect of these processes during a model hindcast of July 2004 was to export 25% more water from the Washington inner shelf past the 100 m isobath, when the plume was included in the model versus when it was not [*Banas et al.*, 2009a].

[36] This net export of water is reflected in a seaward shift in biomass and primary production in the *Banas et al.* [2009b] biophysical model as well. Inclusion of the plume was found to decrease primary production on the inner shelf by 20% under weak to moderate upwelling favorable winds, and simultaneously to increase primary production on the outer shelf and slope by 10–20%. This seaward shift mainly reflects a shift in biomass distribution, rather than a shift in growth rates or spatially integrated production.

[37] Empirical data of macrozooplankton-sized particle distribution and chlorophyll fluorescence from the May 2005 survey [*Peterson and Peterson*, 2008, Figure 1] are consistent with the model results: maximum zooplankton abundance and chlorophyll fluorescence follow the path of the southward tending plume. North of the plume, maximum values occur between the 50 and 100 m isobath. South of the river mouth, the maxima are shifted offshore, extending to the outer shelf and slope. With the available data, however, localized growth and aggregation cannot be distinguished from advective processes. In proximity to the river mouth, aggregations of zooplankton can be pushed across the shelf at velocities up to 38 cm s^{-1}, roughly fivefold faster than typical wind-driven Ekman transport in the region [*Peterson and Peterson*, 2009].

[38] Under some conditions, the plume can also enhance retention of water and biomass [*Hickey and Banas*, 2008]. For example, on the inner shelf north of the river mouth retention typically occurs after a well-developed north tending plume that was formed during a period of downwelling favorable winds moves away from the coast during a subsequent period of upwelling favorable winds: the shoreward plume front forms a barrier to cross-shelf transport. Model studies also suggest [*Banas et al.*, 2009a, 2009b] that interactions between the plume and variable winds episodically retard the equatorward advection of biomass from the Washington shelf, so that the plume acts as a retention feature in an alongcoast sense as well [*Hickey and Banas*, 2008].

5.1.3. Does the Plume Spatially Concentrate Plankton? If So, Where?

[39] Broad-scale and fine-scale surveys with a Triaxus tow body equipped with a Laser Optical Plankton Counter and CTD provided a detailed picture of the relationship between plume waters and macrozooplankton-sized particle distributions. Overall, vertically integrated zooplankton-sized particle abundance and biovolume were elevated in proximity to "aged" plume waters (i.e., surface salinity between 25 and 30). Integrated abundance was approximately 7×10^6 particles m^{-2} in proximity to "aged" plume waters, and 4×10^6 particles m^{-2} outside these areas. In addition, zooplankton tended to aggregate near the surface (upper 10 m) in proximity to river plume waters and were deeper in the water column (25 m) when the plume was not present [*Peterson and Peterson*, 2009].

[40] Analysis of the evolution of salinity following drifters released at the estuary mouth during maximum ebb shows that plume surface water overtakes the plume front [*McCabe et al.*, 2008, 2009], clearly indicating that the front is a surface convergence feature. Fine-scale surveys across the plume front revealed that during a strong ebb tide, zooplankton-sized particles were up to twofold more concentrated on the seaward side of the plume front compared to concentrations 3 km on either side of the front [*Peterson and Peterson*, 2009]. Physical processes associated with the developing plume vertically depressed dense layers of phytoplankton and zooplankton an average of 7 m deeper into the water column both beneath the plume and up to 10 km seaward of the plume front; this feature may be associated with plume-related nonlinear internal waves (see section 5.3.3).

5.1.4. Do Nutrients Supplied by the Plume Enhance Productivity on a Regional Basis?

[41] Nitrate and other nutrients are upwelled onto the shelf seasonally. Upwelling favorable wind stress decreases northward by about a factor of two over the RISE region. RISE nitrate data illustrate that in spite of this decline, nitrate concentrations below the surface layer (~20 m) across the shelf are as high or higher toward the north in the RISE region (Figure 7b). In the upper water column, alongcoast nitrate can be higher to the north or to the south, a result of biological drawdown (Figure 7b).

[42] During periods of strong upwelling favorable winds when the Columbia River plume is directed southwest off the Oregon shelf, upwelled nitrate from the shelf mixed into the plume in the estuary and near the river mouth is the dominant source of nutrients in the plume. During periods of downwelling, when isopycnals and associated high values of nitrate move downward and offshore, this supply route is eliminated. Unlike the Mississippi River, nitrate supply to the plume from its watershed is low in summer [*Conomos et al.*, 1972; *Sullivan et al.*, 2001]. However, in some spring periods, particularly when rainfall is higher than normal, elevated nitrate concentrations from the watershed can be delivered to the ocean by the high river-flow [*Bruland et al.*, 2008]. A seasonal nitrate budget for this region suggests that nitrate input from the Columbia watersheds is two orders of magnitude smaller than input from coastal upwelling, from the Strait of Juan de Fuca or from submarine canyons [*Hickey and Banas*, 2008]. Although small in comparison to other sources on a summer-averaged basis, watershed-derived nutrients may help sustain the ecosystem during periods of delayed seasonal upwelling, as occurred in 2005 [*Hickey and Banas*, 2008] and also during periods of downwelling. Thus, whereas nitrate supply on the Oregon coast is shut off during downwelling or weak winds, the Washington coast has an additional supply from the Columbia River to help maintain productivity during such periods.

[43] Recent measurements indicate that whereas iron can be a limiting nutrient off California [*Hutchins and Bruland*, 1998; *Hutchins et al.*, 1998; *Bruland et al.*, 2001; *Firme et al.*, 2003], phytoplankton growth has not been observed to be iron limited off the Oregon coast [*Chase et al.*, 2002]. RISE studies have shown that iron is not generally limiting on the Washington coast [*Kudela and Peterson*, 2009; *Lohan and Bruland*, 2006, 2008; *Bruland et al.*, 2008]. Not only is the plume from the Columbia heavily laden with iron, particulate iron from the Columbia plume is also

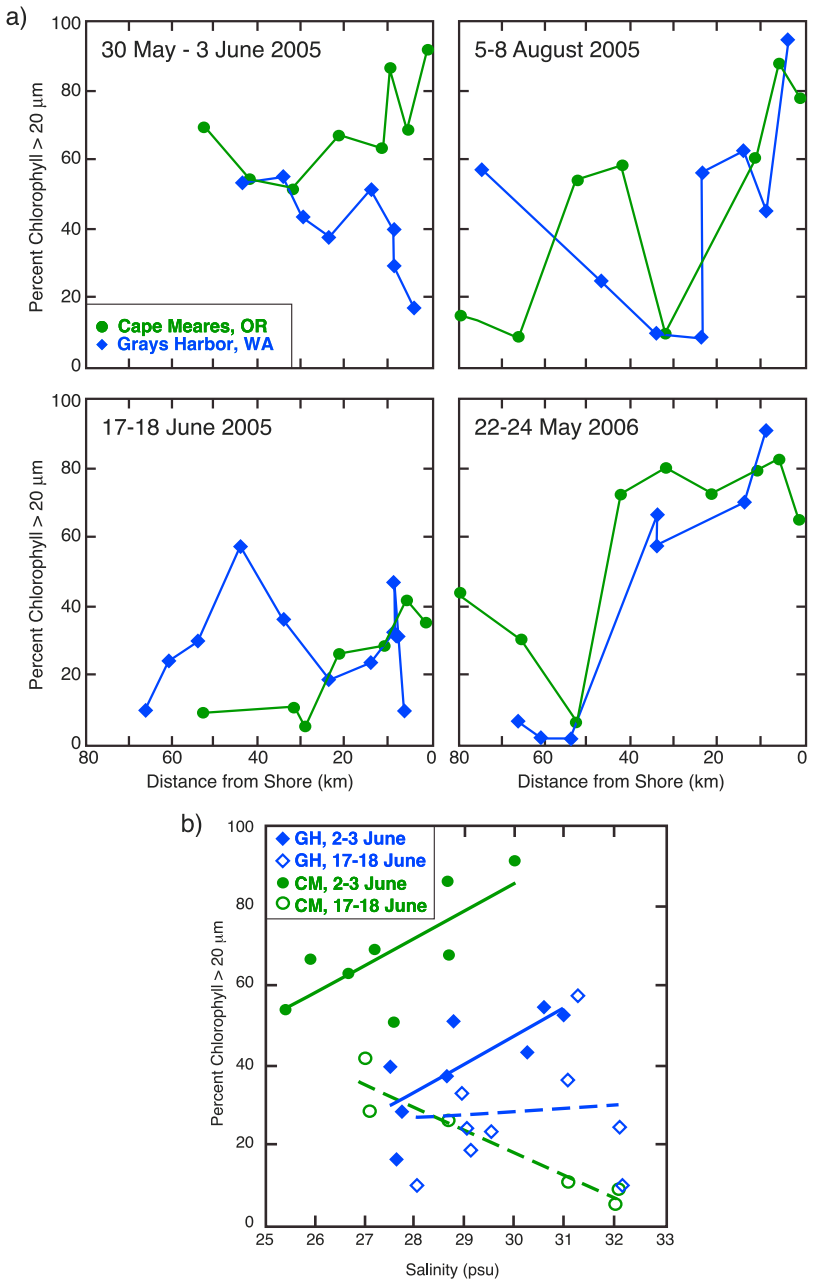

Figure 8. (a) The mean fraction of total chlorophyll greater than 20 μm versus distance offshore on the Washington and Oregon cardinal transects (GH and CM, respectively) during 2005–2006. Location of the Columbia River plume is shown in Figures 7a and 7b. (b) The mean fraction of total chlorophyll greater than 20 μm versus salinity for the Washington (GH) and Oregon (CM) transects during the June 2005 RISE cruise. Data from Kudela Lab.

deposited in midshelf sediments along both the Washington and Oregon coasts. The iron-laden shelf sediment can be mixed into bottom water and thus added to the already nitrate-rich water during coastal upwelling [*Lohan and Bruland*, 2008].

[44] A biological model study comparing results with and without a river plume has shown that more nitrate is provided to the sea surface, and more biomass accumulates in the region near the river mouth when the river plume is present [*Hickey and Banas*, 2008]. The enhancement is due not to the river itself, but to enhanced mixing by the large tidal currents near the river mouth. Similar effects were seen just offshore of Washington's other two coastal estuaries.

5.1.5. Does Phytoplankton Size Differ Between Shelves North and South of the River Mouth?

[45] On three of four RISE cruises size fractionated chlorophyll was measured at >20 μm and total (GF/F; nominally 0.7 μm) sizes. In the RISE region, the >20 μm size fraction is nearly completely dominated by diatoms [*Frame and Lessard*, 2009; *Kudela et al.*, 2006]. The percent >20 μm versus distance offshore on the cardinal transects off Washington and Oregon occupied within 1–2 days of each

other is shown in Figure 8a. The presence or absence of a Columbia plume on these transects is indicated with a gray contour on chlorophyll and nitrate sections in Figures 7a and 7b. The left-hand panels in Figure 8a illustrate cross-shelf structure during periods when the Columbia plume was observed on both transects; the right-hand panels illustrate structure during periods of upwelling, although a plume is present off Oregon (CM transect) during May–June 2006.

[46] Comparison between transects sampled at the start and end of the cruise in May–June 2005 (Figure 8a, left) indicates significant temporal variability over periods of 10–15 days. On that cruise, the percent of large cells within ~30 km of the Oregon coast (CM transect) decreased significantly from 60 to 90% to 25–40% over the 2–3 week period between repeat transect sampling.

[47] Significant spatial differences were observed between Washington and Oregon within 20–30 km of the coast during periods when the Columbia plume was present. In particular, the percent of large cells was smaller off the Washington coast (GH) at most stations (Figure 8a, left). In contrast, during periods when upwelling had recently occurred or was active, the percent of large cells was similar off the two coasts (Figure 8a, right). A two-tail Student's *t* test (assuming unequal variances) applied on all data closer than 25 km from shore, for all four cruises and both Washington (GH) and Oregon (CM) transects (n = 16 and n = 17 for >20 and >5 μm, respectively) gave p = 0.001 and p = 0.018 for the 20 and 5 μm size ranges, respectively, with the percent of large cells higher off Oregon. This is a very conservative test, indicating that the results are highly significant.

[48] Figure 8a also shows that although cell size frequently decreases from nearshore to offshore [*Kudela et al.*, 2006], this pattern was altered in the presence of a plume: cell size appears to increase with distance offshore on the GH transect (upper left panel). This phenomenon is depicted explicitly in Figure 8b, where percent >20 μm is plotted against salinity for the May–June 2005 cruise, during which the plume was observed on all transects. The percent of large cells increases significantly with salinity following the plume as it becomes saltier (i.e., "aging") on the first occupations of both Washington (GH) and Oregon (CM) transects (r = 0.74, 0.75, for CM and GH, respectively, significant at the 95% level), with higher percentages of large cells off Oregon. On the second occupations of these transects, high salinity water (S>31 psu) appeared on the offshore ends of sections (likely originating in the Strait of Juan de Fuca; *MacFadyen et al.* [2008]); the slope of the GH transect data is not significant, and the slope of the CM transect is significant, but negative. These waters were clearly dominated by smaller cells, and the dilution with this new water masked any increase in cell size with aging Columbia plume water in the regression. Based on these data, it appears that size structure is more affected by physical processes (upwelling and plume formation) than by latitude.

5.1.6. Does Turbidity Influence Phytoplankton Photosynthesis?

[49] In contrast to expectations, there was not a strong response in phytoplankton photosynthesis versus irradiance (PE) kinetics from stations within the plume. PE curves collected near surface (2 m) and near bottom in the near-field plume were generally indistinguishable from each other (p>0.05), with more variability between consecutive ebb pulses (temporal variability) than with depth (R. M. Kudela, unpublished data, 2009). In fact, within each cruise, there was a significantly positive relationship between increasing turbidity and increasing maximal chlorophyll-normalized productivity (r = 0.78, significant at the 95% level) (Figure 9). There was also a negative correlation of light transmission with both iron and nitrate concentrations, suggesting that the effects of turbidity on carbon assimilation were either not significant, or were overcome by the co-occurring increase in nutrients. During August 2005 ambient nitrate was in excess of the measured half-saturation parameter for nitrate uptake (Ks) for 5 of 7 PE curves [*Kudela and Peterson*, 2009], while the remaining two stations exhibited elevated carbon assimilation and turbidity (i.e., opposite expectations if the trend is a function of nitrate concentration), suggesting that plume turbidity does not have a negative impact on photosynthesis. Multi-day deckboard incubations during August 2005 also showed no evidence for iron limitation either within or outside the plume [*Kudela and Peterson*, 2009]. Similar results have been reported for plumes in Lake Michigan, where *Lohrenz et al.* [2004] reported no effect on phytoplankton production inside and outside a persistent turbidity plume. Both the Lake Michigan and Columbia River plumes are dominated by particle scattering rather than absorption (e.g., due to colored dissolved material); this appears to result in a high turbidity, diffuse light environment that has relatively little impact on photosynthesizing organisms.

5.1.7. What is the Origin of Plume Turbidity in Spring and Summer?

[50] Detailed measurements of sediment fluxes into and out of the plume in the near-field region highlight an important seasonal trend in the origin of sediment entering the plume [*Spahn et al.*, 2009]. During the spring freshet of May 2006, delivery of sediment to the plume from the river was relatively high and strong vertical stratification prevented sediment from the seabed in the near-field region from entering the plume directly. In contrast, data from the end of the summer in August 2005 show a decrease of input from the river. Under these low flow conditions the near-field plume is much less stratified and strongly interacts with the bottom, generating bottom-attached fronts characterized by elevated turbulence and vertical velocity, which carry resuspended sediment from the seabed toward the surface plume waters. Thus, the data suggest that sediments entering the plume originate primarily from the river in spring and increasingly from the seabed through the summer. This result is consistent with dissolved and labile particulate iron measurements in August 2005 and May 2006, which also show a shift from fluvial to marine sources over the course of the summer [*Bruland et al.*, 2008; S. M. Lippiatt et al., Leachable particulate iron in the Columbia River, estuary and near-field plume, submitted to *Estuarine Coastal Shelf Science*, 2009].

5.2. Regional Plume Structure and Modeling

5.2.1. What is the Spatial and Temporal Extent of the Plume in Spring/Summer?

[51] Three major advancements in our understanding of Columbia plume extent, location and structure were made

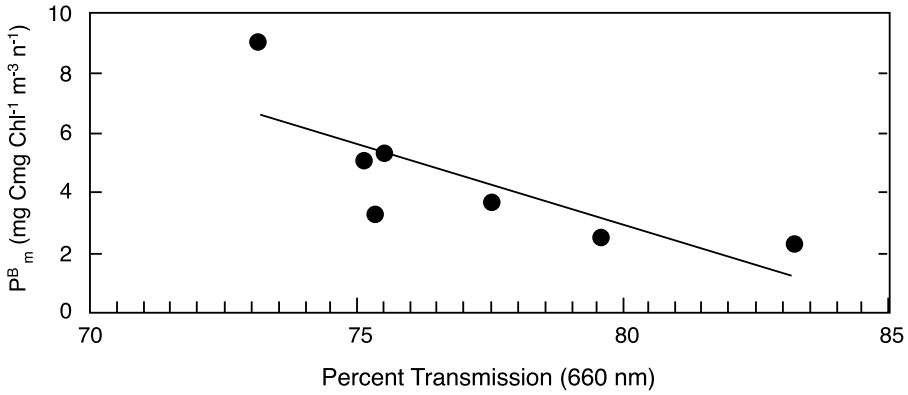

Figure 9. Maximal chlorophyll-normalized productivity (P^B_m) as a function of percent transmission (beam transmissometer; 660 nm) for stations inside the river plume during August 2005. Similar trends were obtained for other years. Photosynthesis irradiance curve data were obtained as described by *Kudela et al.* [2006].

during RISE. First it was demonstrated that in spring, under conditions of high riverflow and strong northward winds, the Columbia can extend the entire length of the Washington coast (~250 km), and then enter the Strait of Juan de Fuca [*Hickey et al.*, 2009]. More important, the plume can interact directly with outflow from the strait, and with the seasonal eddy associated with the strait outflow and the southward shelf break jet. The Columbia plume water becomes entrained in this eddy, subsequently returning southward toward the Columbia mouth, thus extending the residence time of plume water over the shelf by several weeks. A second major finding is that southwest tending plumes often seen in satellite images during upwelling favorable wind conditions can consist primarily of aged water that has spent days or even weeks on the Washington shelf [*Hickey et al.*, 2009; *Liu et al.*, 2009a]. Thus RISE research has shown that the spatial and temporal influence of the plume on the shelf north of the river mouth in spring and summer is much greater than expected from prior data and historical concepts.

[52] A third major advance is the development of a better conceptual view of the structure of the plume. *Garvine* [1982] defined three plume components: the liftoff or source zone, the near field and the far field. As described below, the strongly supercritical, initial advance of the plume has resulted in the need to define new plume water on each tide, bounded by a supercritical front, as the "tidal plume," distinct from the near-field plume [*Horner-Devine et al.*, 2009].

5.2.2. How Well Can We Model Plume Structure and Variability?

[53] The two RISE circulation modeling systems attempt to give realistic simulations of circulation both within the estuary and in the coastal ocean. In spite of this range of scales, and while they differ in details from each other and observations, both modeling systems provide useful insights into circulation dynamics and its response to external forcing [*Liu et al.*, 2009a, 2009b; *MacCready et al.*, 2009; *Burla et al.*, 2009]. In particular, both models capture qualitative changes in plume location, direction and size in response to changes in river discharge and shelf winds. In addition, one of the modeling systems [*Baptista*, 2006] offers both real-time estuary and plume prediction in support of cruises and the opportunity for decadal scale analysis of variability [*Burla et al.*, 2009]. Note that neither model was designed to capture details of the nonhydrostatic tidal plume front and the nonlinear internal waves that develop there [*Nash and Moum*, 2005; L. F. Kilcher and J. D. Nash, Evolution of the Columbia River tidal plume front, manuscript in preparation, 2009].

[54] The ROMS model uses a horizontal resolution of about 400 m in the estuary and plume region, stretching to about 7 km at the far oceanic edges of the domain. Model fields for the summer of 2004 were compared quantitatively with time series from the 3 RISE moorings, 5 CTD sections, HF Radar surface velocity, several tide stations, and a number of moored instruments located within the estuary (maintained by the CORIE/SATURN system). Overall the model data comparison was reasonably good [*MacCready et al.*, 2009; *Liu et al.*, 2009b] with average model skill scores around 0.65, comparable to that of the few other similar studies. Model skill was similar at both tidal and subtidal time scales, and in three regions (the estuary, plume, and shelf). Tidal properties were best modeled within the estuary, while subtidal T and S were best in surface (<20 m depth) plume waters. Plume water properties were reasonably well represented by the model. For the 2004 summer simulation comparisons in the upper 20 m at a mooring in 72 m of water off the Columbia River mouth (Figure 2) the model was on average 1°C too cool, and too fresh by 1 psu [*MacCready et al.*, 2009]. The subtidal RMS error was 1.1°C for T and 1.2 for S, while the tidal RMS error was 0.8°C for T and 1.1 for S [*Liu et al.*, 2009b]. Of greater relevance for the scientific goals of the project, the ROMS model has almost no mean bias in the near surface *stratification*, based on the difference between 1 m and 5 m T and S records [*MacCready et al.*, 2009].

[55] Extensive ROMS experimentation demonstrated the crucial importance of open boundary conditions provided by NCOM and correct bathymetry, such as estuary depth. The NCOM fields on the shelf appeared to have a somewhat deeper thermocline and stronger southward flow than observed [*Liu et al.*, 2009b]. These biases were less apparent in the plume, presumably because of the strong wind and river forcing. While statistical comparisons in the plume are promising, some details of the plume structure are still incorrect. As one example, model surface floats

released near the Columbia River mouth on ebb tide did not penetrate as far seaward as field drifters deployed during RISE observational campaigns [*McCabe et al.*, 2008]. Select numerical experiments also illustrated that float-tracked surface plume water may become too salty (mean salinity excess of ~3–4 psu). Other investigators have found similar results in recent estuarine applications [e.g., *Warner et al.*, 2005; *Li et al.*, 2005]. The tidal plume is characterized by extremely high shear and stratification and remains one of the most difficult to model physical environments in the coastal zone. A hydrostatic model like ROMS necessarily omits details of the plume front and the nonlinear internal waves it generates. Because of this we cannot simulate a potentially large source of observed plume mixing.

[56] The CORIE/SATURN modeling system is built with the philosophy of redundancy in model, grids/domains, and modeling parameterizations. For any given period, daily forecasts and multiyear simulation databases are conducted for at least two domains (river-to-ocean and either estuary-only or estuary/near plume), with river-to-ocean simulations conducted with two models: SELFE [*Zhang and Baptista*, 2008] and ELCIRC [*Zhang et al.*, 2004]; only SELFE is used for the estuary-only and estuary/near plume domains. Simulations often explore multiple parameterizations and the option exists to use model-independent data assimilation strategies [*Frolov et al.*, 2009a] for either improved process understanding [*Frolov et al.*, 2009b] or observational network optimization [*Frolov et al.*, 2008]. Skill assessment has been conducted for simulations based on both ELCIRC [*Baptista et al.*, 2005; *Burla et al.*, 2009] and SELFE [*Zhang and Baptista*, 2008; *Burla et al.*, 2009], and quantitative skill assessment metrics have recently become a part of routine processing of all forecasts and simulation databases in the CORIE/SATURN modeling system (http://www.stccmop.org). Quantitative skill metrics are based on comparisons with both routine CORIE/SATURN observations and observations of opportunity (such as RISE moorings and cruises). Highest skill is typically achieved with SELFE rather than with ELCIRC, and (although often marginally) with hindcasts versus forecasts; during a typical cruise, forecast skill was high enough to direct vessels within 2 km of a predicted concentration more than 55% of the time (Zhang and Baptista, personal communication, 2009).

[57] Typical SELFE/ELCIRC grid resolution is ~150 m in the estuary, 250 m–1 km in the near plume, and 3 km–20 km in the far plume. Skill typically decreases from the estuary to the plume to the shelf outside the near-field plume, reflecting at least in part the different resolution in each of these regions. For the plume, ELCIRC simulations have shown a tendency for excess freshness (e.g., as a relatively extreme example, for 2004 the ELCIRC model bias for salinity at a shelf mooring near the river mouth was −2.9 psu, versus just −0.2 for SELFE) [see *Burla et al.*, 2009]. SELFE was thus the preferred CORIE/SATURN model for both near real-time forecasts in support of oceanographic cruises and the calculation of multiyear time series plume characteristics such as volume, area, thickness and centroid location [*Burla et al.*, 2009].

[58] Although a systematic comparison between the ROMS and SELFE model implementations for the Columbia plume has not been performed to date, examples of their salinity and velocity fields are compared in Figure 10 for (1) a period when the plume tends northward and (2) a period when the plume tends to the southwest. The model runs were selected for dates when CTD transects are available. In addition, satellite imagery (Figure 1) is available within one day of the second model runs. Model maps represent snapshots while CTD data are taken over several hours. For the LB section, total time is 4 h, so that the model output matches the observations between the outer two stations; 2.5 m depth mid shelf current observations at RN, very near the section (see mooring location in Figure 2), show onshore advection during that period, with a possible excursion of less than 2 km between model and CTD data sections. For the CM section, the time elapsed to mid section (mid plume), where models and CTD are contemporaneous, is ~10 h and the distance moved according to mid shelf current observations from that section (see mooring location in Figure 2) is about 6 km offshore, roughly half the distance between a pair of CTD stations.

[59] The side-by-side comparison highlights some qualitative differences between the models. The most dramatic difference is that SELFE salinity structure has much less lateral and vertical structure than that of ROMS; this may be due to lower order numerics and interpolations associated with the semi-Lagrangian time stepping in SELFE. The ROMS plumes in the examples are generally fresher than the SELFE plumes in the plume far field (e.g., the fresh plume tail south of about 46°N in the upper panels). The stronger stratification of the ROMS vertical salinity structure is more consistent with the observations available for these snapshots for both north and southwest plumes. ROMS has much more upwelling at the coast than SELFE—however the deep salinity in ROMS appears consistent with the observations, and more consistent with the observations than the SELFE results. This result may reflect differences in boundary forcing: the smaller domain NRL model used in the ROMS formulation is expected to be more accurate than the larger domain Global NRL model used for SELFE. With respect to the structure of the southwest tending plume, the ROMS plume appears less elongated than the SELFE plume. The blocky shape (for this event at least) of the ROMS plume is consistent with satellite-derived turbidity (see imagery in Figure 1 for one day after the model output). Neither model does very well predicting cross shelf location in these two snapshots: the northward modeled plumes have not spread offshore sufficiently compared to both in situ data and the satellite map; and the southwest tending plumes have spread too far offshore in both models according to the in situ data, even accounting for the several hour timing mismatch between the data and the model results. ROMS does appear to have captured the plume vertical and cross-shelf structure better than SELFE in the upwelling example.

5.2.3. How Well Can We Model Plume Biological Influences?

[60] A four-box (''NPZD'') ecosystem model was designed for the Columbia plume region, parameterized and validated using an array of RISE observations: nutrients, chlorophyll, microzooplankton biomass, phytoplankton community growth and grazing rates, and process studies examining the phytoplankton response to light and

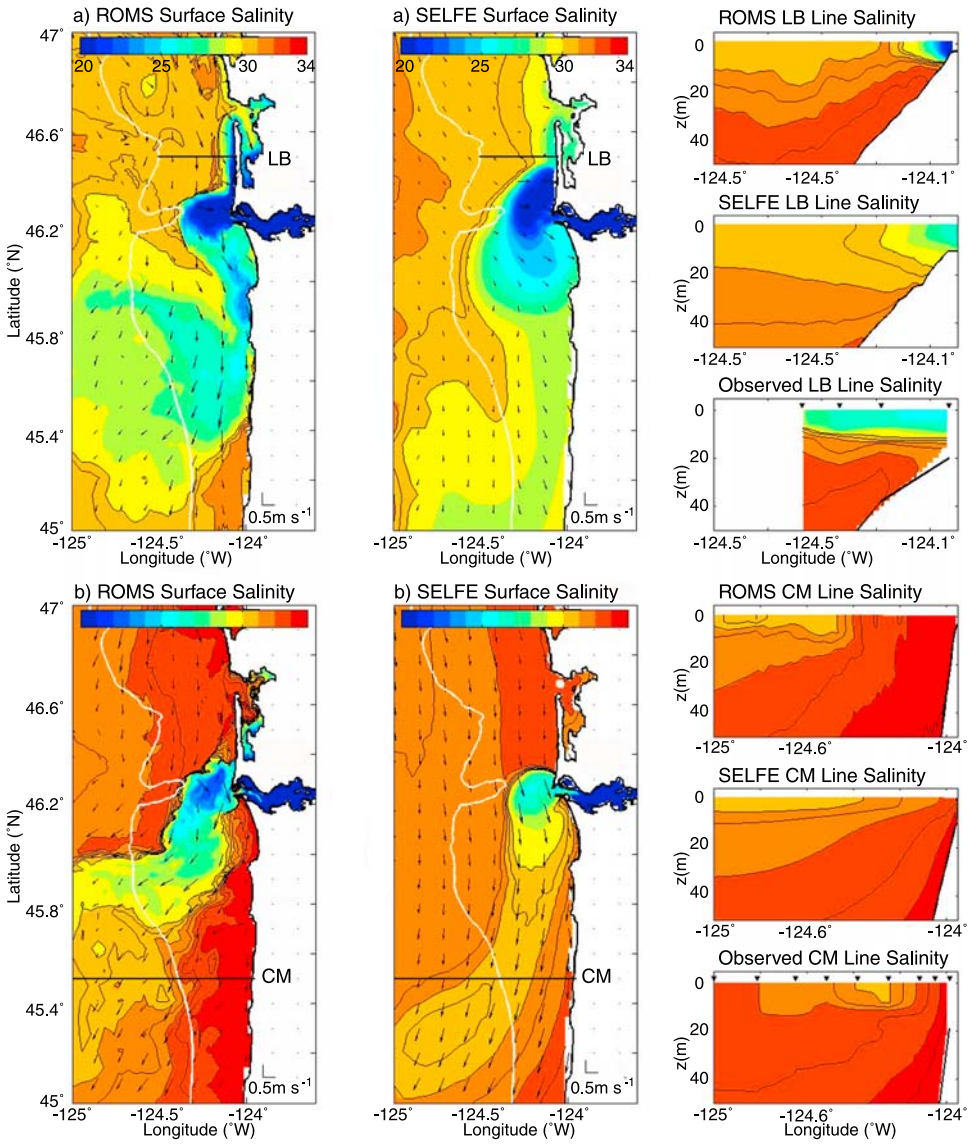

Figure 10. Comparison of surface salinity from two models of the Columbia plume: (left) ROMS [*MacCready et al.*, 2009] and (right) SELFE [*Burla et al.*, 2009] during (a) a downwelling favorable wind period (0000 GMT, 11 June 2005) and (b) an upwelling favorable wind period (0000 GMT, 8 August 2005). The white contour is the 200 m isobath. The setting for the comparison dates is shown in Figure 6 (labeled "M"). On the right hand sides sections from the models are compared with each other and with data taken within 5 h of the model output time. Model results are from MacCready and Baptista Labs; observations from Hickey Lab. A satellite-derived turbidity image obtained one day after the model maps in Figure 10b is shown in Figure 1.

nutrients [*Banas et al.*, 2009b; *Lessard and Frame*, 2008; *Kudela and Peterson*, 2009; Lessard et al., manuscript in preparation, 2009]. The diversity of these observations was key to the modeling effort, a rare opportunity to take an empirical approach to the crucial problem of choosing free parameter values [*Friedrichs et al.*, 2007]. *Banas et al.* [2009b] show that thus parameterized, even a very simple model can pass unusually comprehensive (if not unusually precise) validation tests: to our knowledge this is the first time that an ecosystem model of this type has been compared with extensive simultaneous measurements of phytoplankton and zooplankton biomass and community growth and grazing rates. The model correctly reproduces plume axis profiles of these quantities [*Banas et al.*, 2009b, Figure 8]. Phytoplankton are at moderate levels in the Columbia estuary and peak (in biomass and growth rate) in the near-field to midfield plume, while microzooplankton are low in the estuary and gradually increase until a quasi-equilibrium between growth and grazing is reached in the far-field plume (beyond ~40 km from the mouth). The model likewise reproduces the relationship between the depletion of nutrients and increase in microzooplankton grazing pressure as upwelled water parcels move offshore.

[61] The significance of this model's accurate reproduction of not just stocks (nutrients and biomass) but rates (primary production and microzooplankton grazing) is that

the rates are the real expression of the biological mechanisms and ecosystem dynamics at work in the model. Without a validation of rates and fluxes (as is common, for lack of data), one cannot be sure that stocks are being predicted for the right reasons; with such a validation, we can have confidence in not just the model's mechanistic interpretation but also in hypothetical cases. *Banas et al.* [2009b] also examined a case in which the Columbia River was turned off in order to isolate plume effects on the coastal ecosystem. Two effects of the plume on mean seasonal patterns were found, consistent with observations, as mentioned above (section 5.1): in the cross-shelf direction, a seaward shift in primary production, and in the along-shelf direction, increased retention, which caused a shift toward older communities and increased grazing.

5.3. Mixing Processes, Rates, and Effects

5.3.1. Where Does Mixing of River, Plume, and Oceanic Waters Occur?

[62] Based on analyses of water mass properties [*Bruland et al.*, 2008], turbulence observations [*Nash et al.*, 2009], and the modeled turbulent buoyancy flux (a proxy for mixing of salt and fresh water) of *MacCready et al.* [2009], about half the transformation of fresh to oceanic salinity occurs in the estuary and liftoff or source zone, and half over the shelf. However, the exact partitioning varies significantly with differing wind, tide, and river flow conditions, but generally scales with Ri_E, the estuary Richardson number [*Fischer*, 1972]. Thus, when coastal waters are rich in nutrients, tidal mixing in the plume, estuary and source zone represents a primary mechanism for bringing high-nitrate, high-iron water into the plume. As a result, sufficient nitrate and iron concentrations are established for maximum phytoplankton growth by the time river water reaches the river mouth [*Bruland et al.*, 2008]. *MacCready et al.* [2009] indicate that wind-driven mixing can account for most of the mixing on the shelf during periods of neap tide and strong winds. Whether or not this mechanical forcing is biologically relevant depends on the setting. During upwelling favorable conditions, the southwest tending plume generally overlies, and is surrounded by, nutrient depleted surface waters. In this case intermediate and far-field mixing is unlikely to provide further nutrient input to the plume biomass. On the other hand, northward tending plumes frequently overlie waters with high nitrate, so that wind-driven mixing could aid in fueling production.

5.3.2. What Processes Determine the Plume Structure and Composition?

[63] The tidal plume's initial composition (T, S, N) and vertical structure (thickness and stratification) are largely set by turbulent processes in the estuary [*Cudaback and Jay*, 2000; *Nash et al.*, 2009]. Both observations [*Nash et al.*, 2009] and model energy analyses [*MacCready et al.*, 2009] find turbulent dissipation within the estuary to be primarily driven by the tidal bottom boundary stresses, with only secondary influences from the shear associated with freshwater river flow. As a result, the near-field plume salinity (and other properties such as amount of oceanic nitrate entrained, for example) depends to first order on the balance between freshwater flux (i.e., riverflow Q_f), and turbulent mixing, which scales with the cube of tidal velocity. The process is conveniently described by the estuary Richardson number, which represents a nondimensional ratio of Q_f to u^3. Since the estuary residence time is O(1–5 d), the composition of the tidal plume varies with the neap spring cycle and river flow fluctuations.

[64] As a result of this balance, *Nash et al.* [2009] show that periods of high riverflow and/or weak tides produce relatively thin and highly stratified plumes that detach from the bottom. In contrast, during spring tides and/or weak river flow, plume stratification is reduced, producing a deep river plume that remains in contact with the bottom for up to 5 km beyond the estuary mouth, suspending sediments [*Spahn et al.*, 2009] and blocking coastal flows. Once detached from the bottom, this stratification and thickness control the propagation speed of the tidal plume front as it moves offshore as a buoyant gravity current, its timing and ultimate extent determined by the strength of each ebb pulse [*Jay et al.*, 2009b; L. Kilcher and J. D. Nash, Structure and dynamics of the Columbia River tidal plume front, manuscript in preparation, 2009]. Its three dimensional structure is further modified though coastal currents, which can deflect the plume front, alter its speed, and/or sharpen horizontal gradients; and wind stress, which causes additional and chronic mixing in the aging plume.

[65] The evolution of tidal plume mixing was also explored with drifter data and numerical simulations [*McCabe et al.*, 2008, 2009]. Surface drifters were deployed near the mouth of the Columbia River on a few select ebb tides to track emerging plume water. Conservation equations applied to adjacent drifters determined entrainment rates following plume water as it advected and spread across the shelf. A significant finding is that entrainment continued well beyond liftoff in the "tidal plume interior" as it spreads laterally, suggesting that the spreading process helps maintain vertical mixing as the plume evolves at sea [*McCabe et al.*, 2008]. This observational study further illustrates how differences in plume deceleration, spreading, and thinning lead to entrainment, and qualitatively agrees with ROMS simulations showing significant interior stress and mixing throughout much of the spreading tidal plume [*McCabe et al.*, 2009].

[66] A theoretical model of the initial, supercritical (with respect to the internal Froude number, Fr) expansion of the Columbia tidal plume also shows that the depth of the tidal plume is controlled by a balance between thinning due to plume expansion and thickening due to entrainment [*Jay et al.*, 2009b], echoing the observational analysis of *McCabe et al.* [2008]. Based on the *Jay et al.* [2009b] model, the ratio of mass diffusivity to momentum diffusivity plays a significant role in plume properties, and both the barotropic and baroclinic pressure gradients contribute significantly to the plume momentum balance. Details of tidal plume dynamical balances and how they relate to lateral plume spreading are illustrated with realistic numerical simulations by *McCabe et al.* [2009]. Those authors show that spreading largely results from a competition between the Coriolis force and flow normal pressure gradient, and that plume interior stress is a primary factor acting to slow the plume.

[67] During the ebb that forms each tidal plume, baroclinic shear sustains the gradient Richardson number, $Ri_g \leq 0.25$ within the entire low-salinity surface layer, producing intense turbulence dissipation that scales with the strength of each pulse (Figure 11) [see also *Nash et al.*,

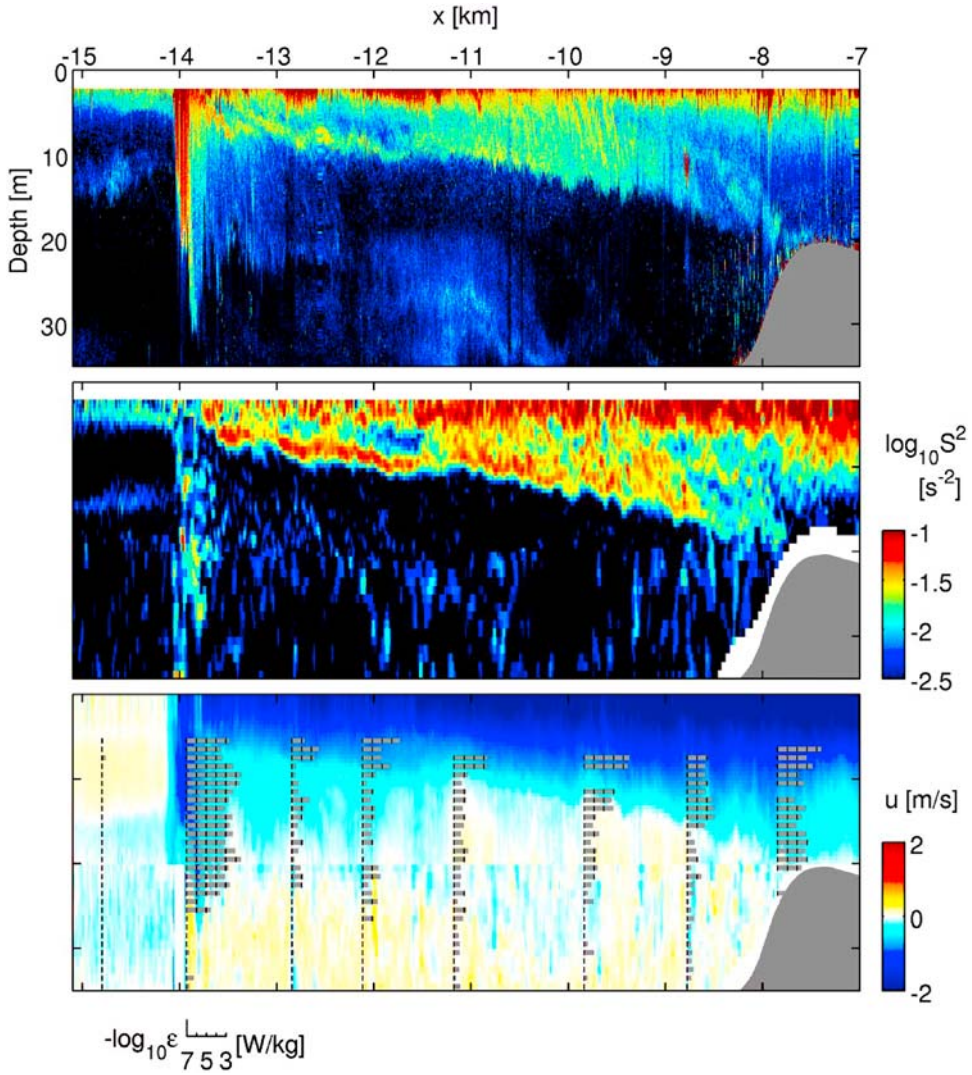

Figure 11. Structure of the tidal plume and turbulent dissipation as revealed through 120 kHz acoustic backscatter (warm colors indicate scattering from turbulence and biology) and ADCP-derived horizontal velocity. (top) Acoustic backscatter, (middle) shear squared (S^2), and (bottom) along-axis velocity (u) during a moderate ebb plume on 8 August 2005. Gray bars (bottom) show turbulent dissipation rate (ε, scale below). Distances are referenced to the river's mouth to the east. This transect was taken along 46°14.4′N. These plots capture liftoff of the tidal plume from the bottom near x = −7.8 km; transition from strongly sheared to layered flow near 11.5 km; and its culmination into a 20 m deep, convergent, and highly turbulent front propagating to the west as a gravity current at 1 m s^{-1} near x = −14 km. Adapted from *Kilcher* [2008].

2009]; strong ebbs are ∼10 times more dissipative than weak ones. In the stratified shear flow inshore of the plume front, turbulence dissipation rates are intense, decaying from $\sim 10^{-3}$ W kg^{-1} near the river mouth to $\sim 10^{-6}$–10^{-5} W kg^{-1} some 20 km offshore (Kilcher and Nash, manuscript in preparation, 2009). Drifter data [*McCabe et al.*, 2008] also confirm that turbulent entrainment continues well after plume liftoff and until the plume becomes geostrophically adjusted, at which point turbulence approaches typical coastal levels. Within fronts, dissipation rates can be significantly higher (Figure 11) [see also *Orton and Jay*, 2005; *Jay et al.*, 2009a; Kilcher and Nash, manuscript in preparation, 2009].

5.3.3. How Do Nonlinear Internal Waves Affect the Mixing at the Columbia River Plume Frontal Region?

[68] Nonlinear internal waves (NLIWs) may be generated when the plume front decelerates beneath the wave speed for wave propagation [*Nash and Moum*, 2005]. *Jay et al.* [2009a] showed that NLIW were most commonly generated on the west and northwest sides of the tidal plume under upwelling favorable or weak wind conditions. They are much less commonly generated during downwelling conditions. Moreover, the front first becomes subcritical (allowing NLIW release) on its south side and southwest sides, regardless of wind direction. This asymmetry is the result of transfer of vorticity to the plume by the underlying tidal

flow. *Pan and Jay* [2009] found that the ambient velocity shear alters the structure of the NLIW by displacing the maximum of the NLIW vertical structure function as much as 5 m below the density interface. This greatly affects NLIW-induced turbulent mixing at the frontal region, because the displaced maximum internal wave shear is at a depth with reduced stability, N^2. An analysis based on observations and internal wave theory suggests that the vertical velocity shear is intensified primarily by the interaction between sheared ambient velocity and the NLIW vertical structure at depths where the combined NLIW and ambient shears result in $Ri_g \leq 0.25$. Typically, neither mechanism acting alone would drive mixing.

5.3.4. How, Where, and When are Phytoplankton Entrained Into the Plume?

[69] Based on the physical and chemical observations, it is clear that most of the turbulent mixing in the plume occurs at the estuary bar and at the tidal plume front, over very short time scales. There was no evidence for distinct plume phytoplankton communities [*Frame and Lessard*, 2009], and no evidence for distinct physiological responses in the plume versus outside the plume [*Kudela and Peterson*, 2009]. This is consistent with the plume entraining and mixing phytoplankton from the near-field coastal waters; while the plume has strikingly different physical and chemical properties, it acts more as biological capacitor (capturing nearshore coastal waters and sometimes adding nutrients), rather than serving as a distinct source or sink for phytoplankton.

5.3.5. Does the Regional Plume Have Multiple Physical, Chemical, or Biological Regions or Layers That Can Be Distinguished?

[70] The water properties of the Columbia plume, which depend on the properties of both river and ocean endmembers as well as the degree of mixing are extremely time-variable as described above. Thus, it is difficult to ascribe specific values of properties to the different plume regions, such as the source region (from the estuary mouth to about 5 km upstream of the mouth), the tidal plume (the pulse of mixed river and shelf water discharged onto the shelf during a single ebb tide; e.g., Figure 11), or the aging plume waters (sometimes referred to as the "far-field" plume). Nevertheless, property gradients are usually sufficiently large that the tidal plume can be readily distinguished from aging plume waters or deep water that has recently upwelled. The tidal plume overlays preexisting or aging plume waters, producing visible layers of salinity, temperature, density and nutrients [*Horner-Devine et al.*, 2009]. Although the estuarine source waters contain freshwater phytoplankton species, because these rapidly die out on encountering oceanic waters, and are replaced by shelf species entrained during mixing, phytoplankton layers are less distinguishable. Significant differences in species composition and diatom composition between plume and oceanic waters have been documented during some plume events [*Frame and Lessard*, 2009].

[71] Although nitrate and much of the dissolved iron is rapidly assimilated by plume phytoplankton, the large excess of these other chemicals in the plume can serve to distinguish the plume. For example, *Aguilar-Islas and Bruland* [2006] demonstrated how elevated silicic acid and dissolved manganese could be used as chemical tracers of the far-field plume. *Brown and Bruland* [2009] showed how elevated dissolved and particulate aluminum in the Columbia River plume could be followed hundreds of km from the river mouth. The dissolved manganese in the Columbia River estuary varies dramatically as a function of spring or neap tides [*Aguilar-Islas and Bruland*, 2006; *Bruland et al.*, 2008]. This can be used to distinguish aged plumes that formed under spring tide conditions from plumes that formed under neap tide conditions.

6. Conclusions

[72] RISE studies have resulted in the development of a new working model of plume processes (Figure 12). The cartoon illustrating this model shows plume processes in plan view as well as along sections emanating from the river mouth and downstream of the mouth. River and tidal waters (1–12 h) are differentiated from aging (1–10 d and upwelling (1–10 d) waters. The cartoon reflects the modern picture of the Columbia plume: a plume with two branches, rather than simply a single southwest plume as depicted in the historic literature [*Hickey et al.*, 2005; *Liu et al.*, 2009a]. The northward branch of the Columbia plume in spring can, on occasion, transit the entire Washington shelf, wrap around the eddy offshore of the Strait of Juan de Fuca and return south to join newly emerging plume waters some 10–20 d later [*Hickey et al.*, 2009].

[73] With respect to the three original RISE hypotheses given in section 1, (1) primary production has been shown to be higher in the newly emerging plume waters than on shelves outside the plume (Figures 12a and 12b) and plume turbidity does not appear to inhibit growth. (2) Model studies demonstrate that cross-shelf export is enhanced by about 20% by the presence of the river plume (Figure 12c). Last, it has been shown that the area both north and south of the river mouth appear to be iron and silicate replete due to the presence of the Columbia plume [*Bruland et al.*, 2008]; in particular, iron limitation on phytoplankton growth is unlikely and diatoms are almost always dominant [*Kudela et al.*, 2006; *Frame and Lessard*, 2009]. This result fundamentally differentiates the northern CCS from coastal waters in the more southern parts of the CCS. No north–south rate differences due to silicate or iron supply were documented.

[74] A number of other important improvements in understanding how freshwater mixes into the coastal ocean and how the resulting plume affects the local ecosystem have emerged from RISE. For example, in situ measurements and model studies demonstrated where mixing occurs and the magnitude of mixing rates, which decrease with distance from the river mouth [*Nash et al.*, 2009; *MacCready et al.*, 2009]. Nonlinear internal waves, generated on the west/northwest side of the plume under upwelling favorable or weak wind conditions (Figure 12c), also affect mixing of plume water [*Jay et al.*, 2009a]. About half the mixing occurs inside the estuary and near the mouth, with the remainder occurring primarily as a result of wind mixing as the plume ages. Nitrate (during upwelling periods) and plankton are both entrained into the plume in the estuary and near mouth mixing; the plume in general does not contain unique phytoplankton assemblages. The river itself can contribute nitrate to the plume with generally low concentrations in summer, and higher concentrations in

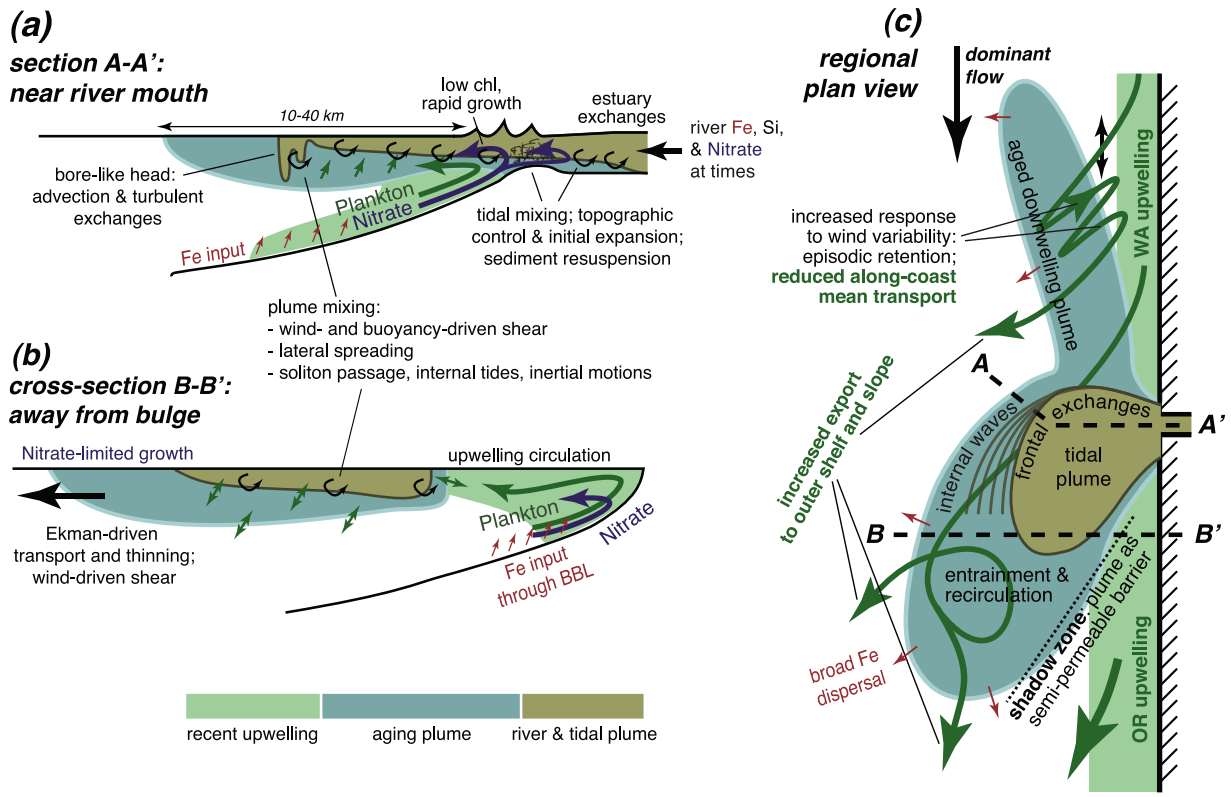

Figure 12. A working model of the processes controlling supply, mixing, and fate of nutrients, phytoplankton, and salt in the vicinity of the Columbia River plume. The age of plume water is color coded (see key). In general, iron, phytoplankton, and nitrate fluxes or pathways are indicated with red, green, and blue arrows, respectively. Black curved arrows indicate mixing; red, single arrows indicate iron flux; green arrows indicate phytoplankton fluxes (single arrow, one way fluxes; double arrow, two way fluxes); the green or blue tracks with arrowheads indicate transport of biomass; black arrows indicate flow.

spring (Figure 12a). Although these amounts are small when seasonally integrated in comparison to that supplied by regional upwelling [*Hickey and Banas*, 2008], they are sufficient to sustain the local ecosystem during periods of extended downwelling or delayed seasonal upwelling [*Bruland et al.*, 2008]. Model results show that tidal dynamics on the shelf near the estuary enhances nitrate supply from the ocean during upwelling events [*Hickey and Banas*, 2008]. Although nitrate supply in the plume is usually moderate to high, phytoplankton become nitrate limited as plume waters age (Figure 12b). With respect to zooplankton, RISE data confirm that macrozooplankton aggregate near Columbia plume fronts [*Peterson and Peterson*, 2009]. Microzooplankton grazing is lowest in the plume, and higher over shelves south of the river mouth than north of it [*Frame and Lessard*, 2009].

[75] The fundamental RISE question was: To what extent is the Columbia River plume the cause of the north–south gradient in chlorophyll concentration in the Pacific Northwest?

[76] RISE confirmed that chlorophyll concentrations are generally higher north of the Columbia mouth than south of it, over the ~150 km between measurement transects (Figure 7a). However, contrary to expectations, growth rates and physiological status of the phytoplankton were similar to the north and south, rather than increasing to the north in conjunction with chlorophyll. One of the most important effects of the Columbia plume on alongcoast gradients is that it acts as a north–south barrier to biomass transport (Figure 12c), deflecting biomass seaward of the Oregon shelf; it channels biomass accumulated on the Washington shelf, much of which originates on the shelf well north of the plume, offshore so that it misses the Oregon shelf. The Oregon shelf essentially has to reset its own phytoplankton community from local upwelling without the addition of an upstream source.

[77] The data clearly demonstrate that upwelling is more frequent and of longer duration off the Oregon coast than off the Washington coast, where wind stress is weaker, and also where plume waters often "cap" upwelling (Figure 12c). Nevertheless, the nitrate supply in shelf bottom waters was always greater to the north (Figure 7b), and is likely due to some combination of remote wind forcing, submarine canyon upwelling enhancement, and the enhanced upwelling near the Strait of Juan de Fuca and its offshore eddy [*Hickey and Banas*, 2008; *MacFadyen et al.*, 2008]. In combination with the higher grazing pressure south of the Columbia river entrance documented in RISE [*Frame and Lessard*, 2009], these data suggest that the northward chlorophyll increase is due to a combination of top-down (grazing) and bottom-up (nitrate) effects, with some partial blocking effect by the plume which makes northern Oregon

a "shadow zone." Although the spatial pattern of grazing likely reflects the influence of the plume [*Banas et al.*, 2009b], enhanced nitrate supply to the northern Washington shelf is not related to the plume.

[78] Thus the Columbia plume does indeed appear to be instrumental in making the southern Washington coast such a rich ecosystem, both through increased nutrient supply or consistency of supply, and increased retention of nutrients and biomass; but the northern source of nutrients and biomass appears to play just as significant a role. Accordingly, to allow quantitative comparison of these processes, models and data collection must expand in scale, to encompass the interactions between freshwater inputs and retention features over hundreds of kilometers of coastline.

[79] **Acknowledgments.** This summary was supported by grant OCE-0239089 to B. Hickey, P. MacCready, and E. Lessard; OCE-0238347 to K. Bruland and R. Kudela; OCE-0238021 to E. Dever; OCE-0238727 to J. Nash and J. Moum; OCE-0237710 to M. Kosro; OCE-0622278 and OCE-0239072 to D. Jay and A. Baptista; and OCE-0239107 to W. Peterson from the National Science Foundation (NSF) as part of the Coastal Ocean Processes RISE Program. The CORIE/SATURN observation and prediction system is scientific infrastructure of the NSF Science and Technology Center for Coastal Margin Observation and Prediction (OCE-0424602) and is also partially supported by regional stakeholders, including the National Oceanic and Atmospheric Administration and the Bonneville Power Administration. The authors would like to thank the captains and crews of the R/V *Wecoma* and *Pt. Sur* for their outstanding support of this research. RISE would not have been successful without the combined efforts of numerous staff and students from each of the research teams; in particular, Nancy Kachel, Susan Geier, Mike Foy, Megan Bernhardt, David Darr, Sherry Palacios, Misty Blakely, Bettina Sohst, Geoffrey Smith, and Keith Leffler. This is contribution 48 of the RISE program. The statements, findings, conclusions, and recommendations are those of the authors and do not necessarily reflect the views of NSF.

References

Aguilar-Islas, A. M., and K. W. Bruland (2006), Dissolved manganese and silicic acid in the Columbia River plume: A major source to the California current and coastal waters off Washington and Oregon, *Mar. Chem.*, *101*(3–4), 233–247, doi:10.1016/j.marchem.2006.03.005.

Bakun, A. (1973), Coastal upwelling indices, west coast of North America, 1946–71, *NOAA Tech. Rep. NMFS SSRF-671*, 103 pp., U.S. Dep. of Commer., Washington, D. C.

Banas, N. S., P. MacCready, and B. M. Hickey (2009a), The Columbia River plume as cross-shelf exporter and along-coast barrier, *Cont. Shelf Res.*, *29*(1), 292–301, doi:10.1016/j.csr.2008.03.011.

Banas, N. S., E. J. Lessard, R. M. Kudela, P. MacCready, T. D. Peterson, B. M. Hickey, and E. Frame (2009b), Planktonic growth and grazing in the Columbia River plume region: A biophysical model study, *J. Geophys. Res.*, *114*, C00B06, doi:10.1029/2008JC004993.

Baptista, A. M. (2006), CORIE: The first decade of a coastal-margin collaborative observatory, in *Oceans 2006*, pp. 1–6, Inst. of Electr. and Electr. Eng., Boston.

Baptista, A. M., Y. Zhang, A. Chawla, M. Zulauf, C. Seaton, E. P. Myers, J. Kindle, M. Wilkin, M. Burla, and P. J. Turner (2005), A cross-scale model for 3D baroclinic circulation in estuary-plume-shelf systems: II. Application to the Columbia River, *Cont. Shelf Res.*, *25*, 935–972, doi:10.1016/j.csr.2004.12.003.

Barnes, C. A., A. C. Duxbury, and B. A. Morse (1972), Circulation and selected properties of the Columbia River effluent at sea, in *The Columbia River Estuary and Adjacent Ocean Waters*, edited by A. T. Pruter and D. L. Alverson, pp. 41–80, Univ. of Wash. Press, Seattle, Wash.

Barron, C. N., A. B. Kara, P. J. Martin, R. C. Rhodes, and L. F. Smedstad (2006), Formulation, implementation and examination of vertical coordinate choices in the global Navy Coastal Ocean Model (NCOM), *Ocean Modell.*, *11*(3–4), 347–375, doi:10.1016/j.ocemod.2005.01.004.

Battisti, D., and B. M. Hickey (1984), Application of remote wind forced coastal trapped wave theory to the Oregon and Washington coasts, *J. Phys. Oceanogr.*, *14*, 887–903, doi:10.1175/1520-0485(1984)014<0887:AORWFC>2.0.CO;2.

Bi, H., R. E. Ruppel, and W. T. Peterson (2007), Modeling the salmon pelagic habitat off the Pacific Northwest (USA) coast using logistic regression, *Mar. Ecol. Prog. Ser.*, *336*, 249–265, doi:10.3354/meps336249.

Boicourt, W. C., W. J. Wiseman Jr., A. Valle-Levinson, and L. P. Atkinson (1998), Continental shelf of the southeastern United States and the Gulf of Mexico: In the shadow of the Western Boundary Current, in *The Sea*, vol. 11, edited by A. R. Robinson and K. H. Brink, pp. 135–182, John Wiley, New York.

Bottom, D. L., C. A. Simenstad, J. Burke, A. M. Baptista, D. A. Jay, K. K. Jones, E. Casillas, and M. H. Schiewe (2005), Salmon at river's end: The role of the estuary in the decline and recovery of Columbia River salmon, *NOAA Tech. Memo., NMFS-NWFSC-68*, 246 pp., U.S. Dep. of Commer., Washington, D. C.

Brown, M. T., and K. W. Bruland (2009), Dissolved and particulate aluminum in the Columbia River and coastal waters of Oregon and Washington: Behavior in near-field and far-field plumes, *Estuarine Coastal Shelf Sci.*, *84*, 171–185, doi:10.1016/j.ecss.2009.05.031.

Bruland, K. W., E. L. Rue, and G. J. Smith (2001), Iron and macronutrients in California coastal upwelling regimes: Implications for diatom blooms, *Limnol. Oceanogr.*, *46*, 1661–1674.

Bruland, K. W., M. C. Lohan, A. M. Aguilar-Islas, G. J. Smith, B. Sohst, and A. Baptista (2008), Factors influencing the chemistry and formation of the Columbia River plume: Nitrate, silicic acid, dissolved Fe and dissolved Mn, *J. Geophys. Res.*, *113*, C00B02, doi:10.1029/2007JC004702.

Burla, M., A. M. Baptista, Y. Zhang, and S. Frolov (2009), Seasonal and interannual variability of the Columbia River plume: A perspective enabled by multiyear simulation databases, *J. Geophys. Res.*, doi:10.1029/2008JC004964, in press.

Chao, S.-Y., and W. C. Boicourt (1986), Onset of estuarine plumes, *J. Phys. Oceanogr.*, *16*, 2137–2149, doi:10.1175/1520-0485(1986)016<2137:OOEP>2.0.CO;2.

Chase, Z., A. van Geen, P. M. Kosro, J. Marra, and P. A. Wheeler (2002), Iron, nutrient, and phytoplankton distributions in Oregon coastal waters, *J. Geophys. Res.*, *107*(C10), 3174, doi:10.1029/2001JC000987.

Chase, Z., P. Strutton, and B. Hales (2007), Iron links river runoff and shelf width to phytoplankton biomass along the U.S. West Coast, *Geophys. Res. Lett.*, *34*, L04607, doi:10.1029/2006GL028069.

Chawla, A., D. A. Jay, A. M. Baptista, M. Wilkin, and C. Seaton (2008), Seasonal variability and estuary-shelf interactions in circulation dynamics of a river-dominated estuary, *Estuaries Coasts*, *31*, 269–288, doi:10.1007/s12237-007-9022-7.

Conomos, T. J., M. G. Gross, C. A. Barnes, and F. A. Richards (1972), River-ocean nutrient relations in summer, in *The Columbia River Estuary and Adjacent Ocean Waters*, edited by A. T. Pruter and D. L. Alverson, pp. 151–175, Univ. of Wash. Press, Seattle, Wash.

Cudaback, C. N., and D. A. Jay (2000), Tidal asymmetry in an estuarine pycnocline: Depth and thickness, *J. Geophys. Res.*, *105*, 26,237–26,252, doi:10.1029/2000JC900135.

Cudaback, C. N., and D. A. Jay (2001), Tidal asymmetry in an estuarine pycnocline: 2. Transport, *J. Geophys. Res.*, *106*(C2), 2639–2652, doi:10.1029/2000JC900151.

Dracup, J. A., and E. Kahya (1994), The relationships between U.S. streamflow and La Niña events, *Water Resour. Res.*, *30*, 2133–2141, doi:10.1029/94WR00751.

Fain, A. M. V., D. A. Jay, D. J. Wilson, P. M. Orton, and A. M. Baptista (2001), Seasonal, monthly and tidal patterns of particulate matter dynamics in the Columbia River estuary, *Estuaries Coasts*, *24*, 770–786, doi:10.2307/1352884.

Firme, G. F., E. L. Rue, D. A. Weeks, K. W. Bruland, and D. A. Hutchins (2003), Spatial and temporal variability in phytoplankton iron limitation along the California coast and consequences for Si, N and C biogeochemistry, *Global Biogeochem. Cycles*, *17*(1), 1016, doi:10.1029/2001GB001824.

Fischer, H. B. (1972), Mass transport mechanisms in partially stratified estuaries, *J. Fluid Mech.*, *53*(4), 671–687, doi:10.1017/S0022112072000412.

Fong, D., and W. R. Geyer (2002), The alongshore transport of fresh water in a surface-trapped river plume, *J. Phys. Oceanogr.*, *32*(3), 957–972, doi:10.1175/1520-0485(2002)032<0957:TATOFI>2.0.CO;2.

Frame, E. R., and E. J. Lessard (2009), Does the Columbia River plume influence phytoplankton community structure along the Washington and Oregon coasts?, *J. Geophys. Res.*, *114*, C00B09, doi:10.1029/2008JC004999.

Friedrichs, M. A. M., et al. (2007), Assessment of skill and portability in regional marine biogeochemical models: Role of multiple planktonic groups, *J. Geophys. Res.*, *112*, C08001, doi:10.1029/2006JC003852.

Frolov, S., A. M. Baptista, and M. Wilkin (2008), Optimizing fixed observational assets in a coastal observatory, *Cont. Shelf Res.*, *28*(19), 2644–2658, doi:10.1016/j.csr.2008.08.009.

Frolov, S., A. M. Baptista, T. Leen, Z. Lu, and R. van der Merwe (2009a), Fast data assimilation using a nonlinear Kalman filter and a model

surrogate: An application to the Columbia River estuary, *Dyn. Atmos. Oceans*, *48*, 16–45, doi:10.1016/jdynatmoce.2008.10.004.

Frolov, S., A. M. Baptista, Y. Zhang, and C. Seaton (2009b), Estimation of ecologically significant circulation features of the Columbia River estuary and plume using a reduced-dimension Kalman filter, *Cont. Shelf Res.*, *29*(2), 456–466, doi:10.1016/j.csr.2008.11.004.

Garcia-Berdeal, I., B. M. Hickey, and M. Kawase (2002), Influence of wind stress and ambient flow on a high discharge river plume, *J. Geophys. Res.*, *107*(C9), 3130, doi:10.1029/2001JC000932.

Garvine, R. W. (1982), A steady state model for buoyant surface plume hydrodynamics in coastal waters, *Tellus*, *34*, 293–306.

Garvine, R. W. (1999), Penetration of buoyant coastal discharge onto the continental shelf: A numerical model experiment, *J. Phys. Oceanogr.*, *29*, 1892–1909, doi:10.1175/1520-0485(1999)029<1892:POBCDO>2.0.CO;2.

Gershunov, A., T. P. Barnett, and D. R. Cayan (1999), North Pacific interdecadal oscillation seen as factor in ENSO-related North American climate anomalies, *Eos Trans. AGU*, *80*(3), 25, doi:10.1029/99EO00019.

Giese, B. S., and D. A. Jay (1989), Modeling tidal energetics of the Columbia River estuary, *Estuarine Coastal Shelf Sci.*, *29*(6), 549–571, doi:10.1016/0272-7714(89)90010-3.

Hamilton, P. (1990), Modeling salinity and circulation for the Columbia River estuary, *Prog. Oceanogr.*, *25*(1–4), 113–156, doi:10.1016/0079-6611(90)90005-M.

Hickey, B. M. (1979), The California current system—Hypotheses and facts, *Prog. Oceanogr.*, *8*, 191–279, doi:10.1016/0079-6611(79)90002-8.

Hickey, B. M. (1989), Patterns and processes of shelf and slope circulation, in *Coastal Oceanography of Washington and Oregon*, edited by M. R. Landry and B. M. Hickey, pp. 41–115, Elsevier Sci., Amsterdam.

Hickey, B. M. (1998), Coastal oceanography of western North America from the tip of Baja California to Vancouver Is, in *The Sea*, vol. 11, edited by K. H. Brink and A. R. Robinson, pp. 345–393, John Wiley, New York.

Hickey, B. M., and N. Banas (2003), Oceanography of the Pacific Northwest coastal ocean and estuaries with application to coastal ecosystems, *Estuaries Coasts*, *26*(48), 1010–1031.

Hickey, B. M., and N. Banas (2008), Why is the northern California Current so Productive?, *Oceanography*, *21*(4), 90–107.

Hickey, B. M., L. J. Pietrafesa, D. A. Jay, and W. C. Boicourt (1998), The Columbia River plume study: Subtidal variability in the velocity and salinity fields, *J. Geophys. Res.*, *103*, 10,339–10,368, doi:10.1029/97JC03290.

Hickey, B. M., S. Geier, N. Kachel, and A. MacFadyen (2005), A bi-directional river plume: The Columbia in summer, *Cont. Shelf Res.*, *25*(14), 1631–1656, doi:10.1016/j.csr.2005.04.010.

Hickey, B. M., A. MacFadyen, W. P. Cochlan, R. M. Kudela, K. W. Bruland, and C. R. Trick (2006), Evolution of biological, chemical and physical water properties in the Pacific Northwest in 2005: Remote or local wind forcing?, *Geophys. Res. Lett.*, *33*, L22S02, doi:10.1029/2006GL026782.

Hickey, B. M., R. McCabe, S. Geier, E. Dever, and N. Kachel (2009), Three interacting freshwater plumes in the northern California Current System, *J. Geophys. Res.*, *114*, C00B03, doi:10.1029/2008JC004907.

Hooff, R. C., and W. T. Peterson (2006), Recent increases in copepod biodiversity as an indicator of changes in ocean and climate conditions in the northern California Current ecosystem, *Limnol. Oceanogr.*, *51*, 2042–2051.

Horner-Devine, A. R. (2009), The bulge circulation in the Columbia River plume, *Cont. Shelf Res.*, *29*(1), 234–251, doi:10.1016/j.csr.2007.12.012.

Horner-Devine, A., D. Fong, S. Monismith, and T. Maxworthy (2006), Laboratory experiments simulating a coastal river inflow, *J. Fluid Mech.*, *555*, 203–232, doi:10.1017/S0022112006008937.

Horner-Devine, A. R., D. A. Jay, P. M. Orton, and E. Spahn (2009), A conceptual model of the strongly tidal Columbia River plume, *J. Mar. Syst.*, *78*, 460–475, doi:10.1016/j.jmarsys.2008.11.025.

Hughes, R. P., and M. Rattray (1980), Salt flux and mixing in the Columbia River estuary, *Estuarine Coastal Mar. Sci.*, *10*, 479–494, doi:10.1016/S0302-3524(80)80070-3.

Hutchins, D. A., and K. W. Bruland (1998), Iron-limited diatom growth and Si:N uptake ratios in a coastal upwelling regime, *Nature*, *393*, 561–564, doi:10.1038/31203.

Hutchins, D. A., G. R. DiTullio, Y. Zhang, and K. W. Bruland (1998), An iron limitation mosaic in the California upwelling regime, *Limnol. Oceanogr.*, *43*, 1037–1054.

Huyer, A., E. J. C. Sobey, and R. L. Smith (1979), The spring transition in currents over the Oregon continental shelf, *J. Geophys. Res.*, *84*(C11), 6995–7011, doi:10.1029/JC084iC11p06995.

Jay, D. A., and J. D. Musiak (1996), Internal tidal asymmetry in channel flows: Origins and consequences, in *Mixing in Estuaries and Coastal Seas, Coastal Estuarine Stud.*, vol. 50, edited by C. Pattiaratchi, pp. 219–258, AGU, Washington, D. C.

Jay, D. A., and J. D. Smith (1990a), Circulation, density distribution and neap-spring transitions in the Columbia River estuary, *Prog. Oceanogr.*, *25*, 81–112, doi:10.1016/0079-6611(90)90004-L.

Jay, D. A., and J. D. Smith (1990b), Residual circulation in shallow estuaries: 1. Highly stratified, narrow estuaries, *J. Geophys. Res.*, *95*(C1), 711–731, doi:10.1029/JC095iC01p00711.

Jay, D. A., and J. D. Smith (1990c), Residual circulation in shallow estuaries: 2. Weakly stratified and partially mixed, narrow estuaries, *J. Geophys. Res.*, *95*(C1), 733–748, doi:10.1029/JC095iC01p00733.

Jay, D. A., J. Pan, P. M. Orton, and A. Horner-Devine (2009a), Asymmetry of Columbia River tidal plume fronts, *J. Mar. Syst.*, *78*, 442–459, doi:10.1016/j.jmarsys.2008.11.015.

Jay, D. A., E. D. Zaron, and J. Pan (2009b), Initial expansion of the Columbia River tidal plume, *J. Geophys. Res.*, doi:10.1029/2008JC004996, in press.

Kay, D. J., and D. A. Jay (2003a), Interfacial mixing in a highly stratified estuary: 1. Characteristics of mixing, *J. Geophys. Res.*, *108*(C3), 3072, doi:10.1029/2000JC000252.

Kay, D. J., and D. A. Jay (2003b), Interfacial mixing in a highly stratified estuary: 2. A "method of constrained differences" approach for the determination of the momentum and mass balances and the energy of mixing, *J. Geophys. Res.*, *108*(C3), 3073, doi:10.1029/2000JC000253.

Kilcher, L. (2008), Turbulence in river plumes, *Oceanography*, *21*(4), 31.

Kosro, P. M. (2005), On the spatial structure of coastal circulation off Newport, Oregon, during spring and summer 2001, in a region of varying shelf width, *J. Geophys. Res.*, *110*, C10S06, doi:10.1029/2004JC002769.

Kosro, P. M., W. T. Peterson, B. M. Hickey, R. K. Shearmann, and S. D. Pierce (2006), Physical versus biological spring transition, *Geophys. Res. Lett.*, *33*, L22S03, doi:10.1029/2006GL027072.

Kudela, R. M., and T. D. Peterson (2009), Influence of a buoyant river plume on phytoplankton nutrient dynamics: What controls standing stocks and productivity?, *J. Geophys. Res.*, *114*, C00B11, doi:10.1029/2008JC004913.

Kudela, R. M., W. Cochlan, T. Peterson, and C. Trick (2006), Impacts on phytoplankton biomass and productivity in the Pacific Northwest during the warm ocean conditions of 2005, *Geophys. Res. Lett.*, *33*, L22S06, doi:10.1029/2006GL026772.

Landry, M. R., and B. M. Hickey (1989), *Coastal Oceanography of Washington and Oregon*, 607 pp., Elsevier Sci., Amsterdam.

Landry, M. R., and C. J. Lorenzen (1989), Abundance, distribution, and grazing impact of zooplankton on the Washington shelf, in *Coastal Oceanography of Washington and Oregon*, edited by M. R. Landry and B. M. Hickey, pp. 175–202, Elsevier Sci., Amsterdam.

Landry, M. R., J. R. Postel, W. K. Peterson, and J. Newman (1989), Broad-scale distributional patterns of hydrographic variables on the Washington/Oregon shelf, in *Coastal Oceanography of Washington and Oregon*, edited by M. R. Landry and B. M. Hickey, pp. 1–40, Elsevier Sci., Amsterdam.

Legaard, K. R., and A. C. Thomas (2006), Spatial patterns in seasonal and interannual variability of chlorophyll and sea surface temperature in the California Current, *J. Geophys. Res.*, *111*, C06032, doi:10.1029/2005JC003282.

Lessard, E. J., and E. R. Frame (2008), The influence of the Columbia River plume on patterns of phytoplankton growth, grazing and chlorophyll on the Washington and Oregon coasts, paper presented at 2008 Ocean Sciences Meeting, Am. Soc. of Limnol. Oceanogr., Orlando, Fla., 2–7 March.

Li, M., L. Zhong, and W. C. Boicourt (2005), Simulations of Chesapeake Bay estuary: Sensitivity to turbulence mixing parameterizations and comparison with observations, *J. Geophys. Res.*, *110*, C12004, doi:10.1029/2004JC002585.

Liu, Y., P. MacCready, and B. M. Hickey (2009a), Columbia River plume patterns as revealed by a hindcast coastal ocean circulation model in summer 2004, *Geophys. Res. Lett.*, *36*, L02601, doi:10.1029/2008GL036447.

Liu, Y., P. MacCready, B. M. Hickey, E. P. Dever, P. M. Kosro, and N. S. Banas (2009b), Evaluation of a coastal ocean circulation model for the Columbia River plume in summer 2004, *J. Geophys. Res.*, *114*, C00B04, doi:10.1029/2008JC004929.

Lohan, M. C., and K. W. Bruland (2006), Importance of vertical mixing for additional sources or nitrate and iron to surfaces waters of the Columbia River plume: Implications for biology, *Mar. Chem.*, *98*, 260–273, doi:10.1016/j.marchem.2005.10.003.

Lohan, M. C., and K. W. Bruland (2008), Elevated Fe (II) and total dissolved Fe in hypoxic shelf waters off the coast of Washington and Oregon: An enhanced source of iron to coastal upwelling regimes, *Environ. Sci. Technol.*, *42*(17), 6462–6468, doi:10.1021/es800144j.

Lohrenz, S. E., G. L. Fahnenstiel, D. F. Millie, O. M. E. Schofield, T. Johengen, and T. Bergmann (2004), Spring phytoplankton photosynthesis, growth, and primary production and relationships to a recurrent sediment plume and river inputs in southeastern Lake Michigan, *J. Geophys. Res.*, *109*, C10S14, doi:10.1029/2004JC002383.

MacCready, P., N. S. Banas, B. M. Hickey, E. P. Dever, and Y. Liu (2009), A model study of tide- and wind-induced mixing in the Columbia River estuary and plume, *Cont. Shelf Res.*, *29*(1), 278–291, doi:10.1016/j.csr.2008.03.015.

MacFadyen, A., B. M. Hickey, and M. G. G. Foreman (2005), Transport of surface waters from the Juan de Fuca Eddy region to the Washington coast: Implications for HABs, *Cont. Shelf Res.*, *25*, 2008–2021, doi:10.1016/j.csr.2005.07.005.

MacFadyen, A., B. M. Hickey, and W. P. Cochlan (2008), Influences of the Juan de Fuca Eddy on circulation, nutrients, and phytoplankton production in the northern California Current System, *J. Geophys. Res.*, *113*, C08008, doi:10.1029/2007JC004412.

Mantua, N. J., S. R. Hare, Y. Zhang, J. M. Wallace, and R. C. Francis (1997), A Pacific interdecadal climate oscillation with impacts on salmon production, *Bull. Am. Meteorol. Soc.*, *78*, 1069–1079, doi:10.1175/1520-0477(1997)078<1069:APICOW>2.0.CO;2.

Mass, C., et al. (2003), Regional environmental prediction over the Pacific Northwest, *Bull. Am. Meteorol. Soc.*, *84*, 1353–1366, doi:10.1175/BAMS-84-10-1353.

McCabe, R., B. Hickey, and P. MacCready (2008), Observational estimates of entrainment and vertical salt flux behind the frontal boundary of a spreading river plume, *J. Geophys. Res.*, *113*, C08027, doi:10.1029/2007JC004361.

McCabe, R. M., P. MacCready, and B. M. Hickey (2009), Ebb tide dynamics and spreading of a large river plume, *J. Phys. Oceanogr.*, *39*, 2839–2856, doi:10.1175/2009JPO4061.1.

Morgan, C. A., A. De Robertis, and R. W. Zabel (2005), Columbia River plume fronts: I. Hydrography, zooplankton distribution, and community composition, *Mar. Ecol. Prog. Ser.*, *299*, 19–31, doi:10.3354/meps299019.

Nash, J. D., and J. N. Moum (2005), River plumes as a source of large-amplitude internal waves in the coastal ocean, *Nature*, *437*, 400–403, doi:10.1038/nature03936.

Nash, J. D., L. Kilcher, and J. N. Moum (2009), Structure and composition of a strongly stratified, tidally pulsed river plume, *J. Geophys. Res.*, *114*, C00B12, doi:10.1029/2008JC005036.

Nittrouer, C. A. (1978), The process of detrital sediment accumulation in a continental shelf environment: An examination of the Washington shelf, Ph.D. dissertation, 243 pp., Univ. of Washington, Seattle, Wash.

Orton, P. M., and D. A. Jay (2005), Observations at the tidal plume front of a high volume river outflow, *Geophys. Res. Lett.*, *32*, L11605, doi:10.1029/2005GL022372.

Pan, J., and D. A. Jay (2009), Effects of ambient velocity shear on internal solitons and associated mixing at the Columbia River front, *J. Geophys. Res.*, *114*, C00B07, doi:10.1029/2008JC004988.

Pearcy, W. G. (1992), *Books in Recruitment Fishery Oceanography: Ocean Ecology of North Pacific Salmonids*, 179 pp., Univ. of Wash. Press, Seattle, Wash.

Peterson, J. O., and W. T. Peterson (2008), Influence of the Columbia River plume (USA) on the vertical and horizontal distribution of mesozooplankton over the Washington and Oregon shelf, *ICES J. Mar. Sci.*, *65*, 477–483, doi:10.1093/icesjms/fsn006.

Peterson, J. O., and W. T. Peterson (2009), The influence of the Columbia River plume on cross-shelf transport of zooplankton, *J. Geophys. Res.*, *114*, C00B10, doi:10.1029/2008JC004965.

Pierce, D. P., J. A. Barth, R. E. Thomas, and G. W. Fleischer (2006), Anomalously warm July 2005 in the northern California Current: Historical context and the significance of cumulative wind stress, *Geophys. Res. Lett.*, *33*, L22S04, doi:10.1029/2006GL027149.

Pruter, A. T., and D. L. Alverson (1972), *The Columbia River Estuary and Adjacent Coastal Waters*, 868 pp., Univ. of Wash. Press, Seattle, Wash.

Roegner, C., B. M. Hickey, J. Newton, A. Shanks, and D. Armstrong (2002), Estuarine-nearshore links during a coastal upwelling cycle: Plume and bloom intrusions into Willapa Bay, Washington, *Limnol. Oceanogr.*, *47*(4), 1033–1042.

Shaw, T. C., L. R. Feinberg, and W. T. Peterson (2009), Interannual variations in vital rates of copepods and euphausiids during the RISE study 2004–2006, *J. Geophys. Res.*, *114*, C00B08, doi:10.1029/2008JC004826.

Shulman, I., J. C. Kindle, S. deRada, S. C. Anderson, B. Penta, and P. J. Martin (2004), Development of a hierarchy of nested models to study the California Current System, in *Estuarine and Coastal Modeling: Proceedings of 8th International Conference on Estuarine and Coastal Modeling*, edited by M. L. Spaulding, pp. 74–88, Am. Soc. of Civ. Eng., Reston, Va.

Simenstad, C. A., L. Small, C. D. McIntire, D. A. Jay, and C. R. Sherwood (1990a), Columbia River estuary studies: An introduction to the estuary, a brief history, and prior studies, *Prog. Oceanogr.*, *25*, 1–14, doi:10.1016/0079-6611(90)90002-J.

Simenstad, C. A., C. D. McIntire, and L. F. Small (1990b), Consumption processes and food web structure in the Columbia River estuary, *Prog. Oceanogr.*, *25*, 271–298, doi:10.1016/0079-6611(90)90010-Y.

Small, L. F., C. D. McIntire, K. B. Macdonald, J. R. Laralara, B. E. Frey, M. C. Amspoker, and T. Winfield (1990), Primary production, plant and detrital biomass, and particle transport in the Columbia River estuary, *Prog. Oceanogr.*, *25*, 175–210, doi:10.1016/0079-6611(90)90007-O.

Spahn, E. Y., A. R. Horner-Devine, D. A. Jay, J. Nash, and L. Kilcher (2009), Particle re-suspension in the Columbia River plume near field, *J. Geophys. Res.*, *114*, C00B14, doi:10.1029/2008JC004986.

Strub, P. T., J. S. Allen, A. Huyer, and R. L. Smith (1987), Large-scale structure of the spring transition in the coastal ocean off western North America, *J. Geophys. Res.*, *92*(C2), 1527–1544, doi:10.1029/JC092iC02p01527.

Strub, P. T., C. James, A. C. Thomas, and M. R. Abbott (1990), Seasonal and nonseasonal variability of satellite-derived surface pigment concentration in the California Current, *J. Geophys. Res.*, *95*, 11,501–11,530, doi:10.1029/JC095iC07p11501.

Sullivan, B. E., F. G. Prahl, L. F. Small, and P. A. Covert (2001), Seasonality of phytoplankton production in the Columbia River: A natural or anthropogenic pattern?, *Geochim. Cosmochim. Acta*, *65*, 1125–1139, doi:10.1016/S0016-7037(00)00565-2.

Swartzman, G. L. (2001), Spatial patterns of hake (*merluccius productus*) shoals and euphausiid patches in the California current ecosystem, in *Spatial Processes and Management of Marine Populations*, edited by G. H. Kruse et al., pp. 495–512, Univ. of Alaska Sea Grant College Program, Fairbanks, Alaska.

Swartzman, G., and B. Hickey (2003), Evidence for a regime shift after the 1997–1998 El Niño, based on 1995, 1998 and 2001 acoustic surveys in the Pacific Eastern Boundary Current, *Estuaries*, *26*(4), 1032–1043, doi:10.1007/BF02803361.

Thomas, A. C., and R. Weatherbee (2006), Satellite-measured temporal variability of the Columbia River plume, *Remote Sens. Environ.*, *100*, 167–178, doi:10.1016/j.rse.2005.10.018.

Thomas, A. C., M. E. Carr, and P. T. Strub (2001), Chlorophyll variability in eastern boundary Currents, *Geophys. Res. Lett.*, *28*, 3421–3424, doi:10.1029/2001GL013368.

Venegas, R., P. Strub, E. Beier, R. Letelier, A. Thomas, T. Cowles, C. James, L. Soto-Mardones, and C. Cabrera (2008), Satellite-derived variability in chlorophyll, wind stress, sea surface height, and temperature in the northern California Current system, *J. Geophys. Res.*, *113*, C03015, doi:10.1029/2007JC004481.

Ware, D. M., and R. E. Thomson (2005), Bottom-up ecosystem trophic dynamics determine fish production in the Northeast Pacific, *Science*, *308*(5726), 1280–1284, doi:10.1126/science.1109049.

Warner, J. C., W. R. Geyer, and J. A. Lerczak (2005), Numerical modeling of an estuary: A comprehensive skill assessment, *J. Geophys. Res.*, *110*, C05001, doi:10.1029/2004JC002691.

Wiseman, W. J., and R. W. Garvine (1995), Plumes and coastal currents near large river mouths, *Estuaries Coasts*, *18*(3), 509–517, doi:10.2307/1352368.

Wolter, K., and M. S. Timlin (1993), Monitoring ENSO in COADS with a seasonally adjusted principal component index, paper presented at 17th Climate Diagnostics Workshop, NOAA, Norman, Okla.

Yankovsky, A. E., B. M. Hickey, and A. K. Munchow (2001), Impact of variable inflow on the dynamics of a coastal buoyant plume, *J. Geophys. Res.*, *106*, 19,809–19,824, doi:10.1029/2001JC000792.

Zhang, Y., and A. M. Baptista (2008), SELFE: A semi-implicit Eulerian-Lagrangian finite-element model for cross-scale ocean circulation, *Ocean Modell.*, *21*(3–4), 71–96, doi:10.1016/j.ocemod.2007.11.005.

Zhang, Y., A. M. Baptista, and E. P. Myers (2004), A cross-scale model for 3D baroclinic circulation in estuary-plume-shelf systems: I. Formulation and skill assessment, *Cont. Shelf Res.*, *24*(18), 2187–2214, doi:10.1016/j.csr.2004.07.021.

N. S. Banas, Applied Physics Laboratory, University of Washington, Seattle, WA 98195, USA.

A. M. Baptista, Science and Technology Center for Coastal Margin Observation and Prediction, Oregon Health and Science University, Beaverton, OR 97006, USA.

K. W. Bruland and R. M. Kudela, Department of Ocean Sciences, University of California, Santa Cruz, CA 95064, USA.

E. P. Dever, L. K. Kilcher, P. M. Kosro, J. D. Nash, and J. O. Peterson, College of Ocean and Atmospheric Sciences, Oregon State University, Corvallis, OR 97331, USA.

B. M. Hickey, E. J. Lessard, and P. MacCready, School of Oceanography, University of Washington, Seattle, WA 98195, USA. (bhickey@u.washington.edu)

A. R. Horner-Devine, Civil and Environmental Engineering, University of Washington, Seattle, WA 98195, USA.

D. A. Jay, J. Pan, and E. D. Zaron, Civil and Environmental Engineering, Portland State University, Portland, OR 97207, USA.

M. C. Lohan, SEOS, University of Plymouth, Plymouth, UK.

R. M. McCabe, Department of Aviation, University of New South Wales, Sydney, NSW 2052, Australia.

P. M. Orton, Lamont-Doherty Earth Observatory, Earth Institute at Columbia University, Palisades, NY 10964, USA.

W. T. Peterson, Northwest Fisheries Science Center, NOAA Fisheries, Newport, OR 97365, USA.